NAVAL POSTGRADUATE SCHOOL

MONTEREY, CALIFORNIA

THESIS

A LASER METROLOGY SYSTEM FOR PRECISION POINTING

by

Edward J. Hospodar, Jr.

December 2003

Thesis Advisor:	Brij N. Agrawal
Second Reader:	Hong-Jen Chen

Approved for public release; distribution is unlimited

THIS PAGE INTENTIONALLY LEFT BLANK

REPORT DOCUMENTATION PAGE		Form Approved OMB No. 0704-0188

1. AGENCY USE ONLY *(Leave blank)*	2. REPORT DATE	3. REPORT TYPE AND DATES COVERED
	December 2003	Master's Thesis

4. TITLE AND SUBTITLE: Laser Metrology System for Precision Pointing	5. FUNDING NUMBERS
6. AUTHOR(S) Edward J. Hospodar, Jr.	
7. PERFORMING ORGANIZATION NAME(S) AND ADDRESS(ES) Naval Postgraduate School Monterey, CA 93943-5000	8. PERFORMING ORGANIZATION REPORT NUMBER
9. SPONSORING /MONITORING AGENCY NAME(S) AND ADDRESS(ES) N/A	10. SPONSORING/MONITORING AGENCY REPORT NUMBER

11. SUPPLEMENTARY NOTES The views expressed in this thesis are those of the author and do not reflect the official policy or position of the Department of Defense or the U.S. Government.

12a. DISTRIBUTION / AVAILABILITY STATEMENT	12b. DISTRIBUTION CODE
Approved for public release; distribution is unlimited	

13. ABSTRACT (maximum 200 words)

Precision spacecraft payloads are driving the need for fine pointing control and vibration cancellation. One implementation that provides pointing and disturbance control is the Stewart-Gough platform equipped with active sensing and actuating elements. The Precision Pointing Hexapod (PPH) at Naval Postgraduate School (NPS) is exactly such a platform initially installed with voice coil actuators and accelerometers on each strut by CSA Engineering Inc. High pointing accuracy, however, requires an additional external sensing system that feeds back the accurate location and orientation information of the moving platform for control.

The first implementation by NPS of such sensing system is the eddy current metrology system. Currently, that system only provides measurement of the two degrees of motion that define the pointing direction and has issues such as questionable absolute pointing accuracy and lower resolution. This thesis seeks to develop a new laser metrology system, utilizing diode lasers and position sensing detectors, to provide all six degree of freedom information of the platform motion at higher precision and accuracy. The tasks of developing the laser metrology system from theory to design, fabrication, implementation, and verification are documented in this thesis. Recommendations for future work and lessons learned are also captured.

14. SUBJECT TERMS Precision Pointing Hexapod, Stewart-Gough Platform, Stewart-Platform, PSD, Laser	15. NUMBER OF PAGES 81
	16. PRICE CODE

17. SECURITY CLASSIFICATION OF REPORT	18. SECURITY CLASSIFICATION OF THIS PAGE	19. SECURITY CLASSIFICATION OF ABSTRACT	20. LIMITATION OF ABSTRACT
Unclassified	Unclassified	Unclassified	UL

NSN 7540-01-280-5500

Standard Form 298 (Rev. 2-89)
Prescribed by ANSI Std. 239-18

THIS PAGE INTENTIONALLY LEFT BLANK

Approved for public release; distribution is unlimited

A LASER METROLOGY SYSTEM FOR PRECISION POINTING

Edward J. Hospodar, Jr.
Major, United States Air Force
B.S., U.S. Air Force Academy, 1993

Submitted in partial fulfillment of the
requirements for the degree of

MASTER OF SCIENCE IN ASTRONAUTICAL ENGINEERING

from the

NAVAL POSTGRADUATE SCHOOL
December 2003

Author: Edward J. Hospodar, Jr.

Approved by: Brij N. Agrawal
Thesis Advisor

Hong-Jen Chen
Second Reader

Anthony J. Healey
Chairman, Department of Mechanical and Astronautical Engineering

THIS PAGE INTENTIONALLY LEFT BLANK

ABSTRACT

Precision spacecraft payloads are driving the need for fine pointing control and vibration cancellation. One implementation that provides pointing and disturbance control is the Stewart-Gough platform equipped with active sensing and actuating elements. The Precision Pointing Hexapod (PPH) at Naval Postgraduate School (NPS) is exactly such a platform initially installed with voice coil actuators and accelerometers on each strut by CSA Engineering Inc. High pointing accuracy, however, requires an additional external sensing system that feeds back the accurate location and orientation information of the moving platform for control.

The first implementation by NPS of such sensing system is the eddy current metrology system. Currently, that system only provides measurement of the two degrees of motion that define the pointing direction and has issues such as questionable absolute pointing accuracy and lower resolution. This thesis seeks to develop a new laser metrology system, utilizing diode lasers and position sensing detectors, to provide all six degree of freedom information of the platform motion at higher precision and accuracy. The tasks of developing the laser metrology system from theory to design, fabrication, implementation, and verification are documented in this thesis. Recommendations for future work and lessons learned are also captured.

THIS PAGE INTENTIONALLY LEFT BLANK

TABLE OF CONTENTS

LIST OF FIGURES

LIST OF TABLES

THIS PAGE INTENTIONALLY LEFT BLANK

ACKNOWLEDGMENTS

Thanks to Brij Agrawal for providing guidance, resources and enough freedom for this to be my own project. Thanks to Hong-Jen Chen for his thorough attention to detail and for sharing his engineering expertise. His efforts turned the ideas into a system and helped me learn Eastern ways of thinking about problems. Thanks to Sam Barone for helping me with the alignment. Thanks to Jay Adeff and Glenn Harrell for taking this thesis off the blackboard and into the shop to give it physical form. Thanks to Brian Moore and Vinny Watson, fellow SRDC, who helped me on numerous tasks. Finally, thanks to Andres Larraza for setting me up with my first thesis, and for the good sense to know when it was time to cut losses and transition to new research.

THIS PAGE INTENTIONALLY LEFT BLANK

I. INTRODUCTION

A. MOTIVATION

In the space industry cost and mission performance place a great emphasis on the control of rigid and flexible spacecraft bodies. As control requirements have become more stringent, improvements have been made in controllers, actuators, and sensors. In order to meet these requirements, optical measurement (metrology) has become an important sensing technique for fine control. For spacecraft, liquid-filled inclinometers cannot be used due to their gravity and temperature dependence and limited resolution, and eddy current sensors are undesirable due to electromagnetic compatibility with the rest of the spacecraft. Optical (laser) metrology is a feasible sensor option because it does not have these limitations, and it has excellent resolution that is necessary for pointing of flexible optical payloads.

B. OBJECTIVES

The focus of this research is to develop and implement an optical metrology system for the Naval Postgraduate School (NPS) Precision Pointing Hexapod (PPH) that builds upon the research of previous students [Ref 1,2]. The NPS PPH, hereafter referred to as the “PPH”, is a testbed for precision pointing control and vibration isolation. The PPH already has a metrology system made up of eddy current sensors that measure the tip and tilt of the PPH—two degrees of freedom. The goal of the optical metrology system is to measure the complete position and orientation of the PPH (all six degrees of freedom)—and to improve the precision and accuracy of data that is supplied to the controller.

Achieving the objective requires development of a mathematical representation of the metrology system and simplifying assumptions; design and fabrication of a mechanical system to mount the laser metrology; design, development, and fabrication of alignment and verification tools and procedures; and integration of the laser metrology sensor measurements into the controller. Theoretically, the laser metrology system can make more precise measurements

than the eddy current metrology system. This thesis is an attempt to take advantage of the gain in precision while recognizing that the accuracy of the implemented laser metrology system will always be less than the theoretical precision.

C. BACKGROUND

The advent of light-weight, low power, solid state lasers coupled with high resolution, high speed response, highly reliable light detectors makes optical metrology quite feasible for spacecraft applications. In conjunction with control law software and the actuators of the PPH, the optical metrology system completes the control system of the PPH.

1. PPH Overview

The PPH is parallel manipulator known as a Stewart-Gough platform. It is a six-legged apparatus connecting a fixed base to a moving platform. The six legs expand and contract to induce or actuate the motion. In this paper, the fixed base is known as the “lower plate” and can be considered attached to the spacecraft. The moving platform is known as the “upper plate” and is the platform upon which a sensitive payload would be attached.

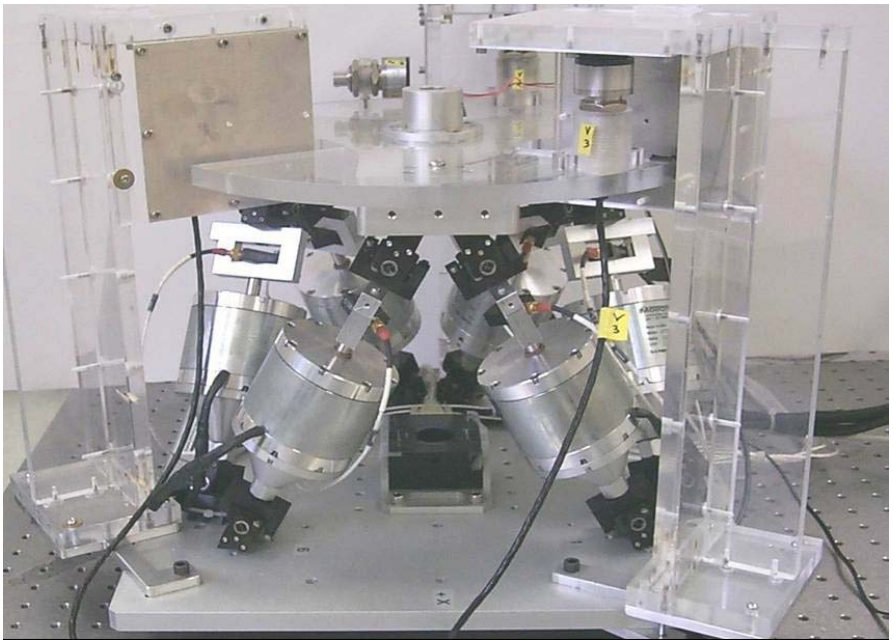

Figure 1. PPH

The optical metrology system measures the location of the upper plate and it's orientation in reference to some known location on the spacecraft, in this case, the lower plate. Disturbances can originate in the spacecraft or in the payload. Examples of disturbances generated by the spacecraft include, the solar array drive assembly motor, spinning of the reaction wheels, firing of thrusters, and the vibration of other large appendages like solar array flapping. The payload can also have disturbances due to cooler pumping and thermal transients. A shaker on the bottom plate simulates disturbances caused by the spacecraft. Similarly, attaching a shaker to the top plate can generate disturbances by the payload on itself. The PPH includes the entire control architecture—sensor, controller, and actuator. However, the purpose of this thesis is to go into detail on the metrology system. Therefore, further discussion is scoped to what is germane to the metrology system.

2. Choices for Sensor

One common element in optical metrology is a photo-detector. The engineer can choose between a Charge Coupled Device (CCD) and a Position Sensitive Detector (PSD). In useful terms, the CCD is divided into pixels with each pixel able to detect light. The benefit of a CCD is that multiple light measurements can be made simultaneously on the CCD. The drawback of the CCD is that spatial resolution is usually limited by the size of the pixel. Cost increases as spatial resolution improves (ever smaller pixels). CCD pixel sizes smaller than 1 micron are quite expensive. Conversely, the PSD has the disadvantage of only being able to make single light measurements, so multiple PSD's are necessary to detect and measure multiple light sources. The benefit of the PSD is it's excellent resolution for the price. PSD resolution below a micron is commonly available for hundreds of dollars [Ref 3]. This thesis requires both low cost and excellent spatial resolution, so PSD's are used in the laser metrology system, although more expensive CCD's were also considered in another candidate architecture that was not implemented. Additionally, the PSD offers greater precision than the Eddy Current metrology system that exists on the PPH.

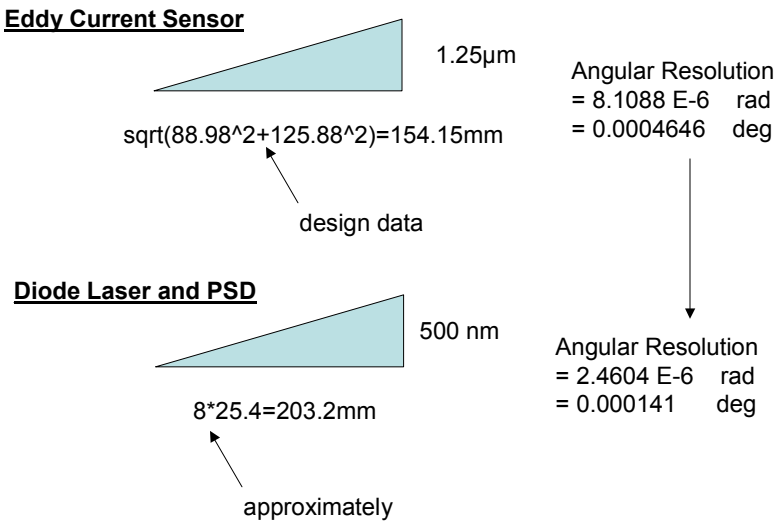

Figure 2. Theoretical Improvement in Precision by Switching to Laser Metrology

3. How a PSD Works

Since PSD's will be used as the detector throughout the rest of this thesis, some basic principles of the PSD will be explained up front. A PSD works on the basis of a P-N junction. A uniform resistive layer is formed on the surfaces of a high-resistivity semi-conductor substrate, and a pair of electrodes formed on both ends of the resistive layer extracts the current [Ref 4]. Knowledge of the current and the resistance allows for the determination of the voltage. Voltage is converted to displacement by a calibrated linear relationship.

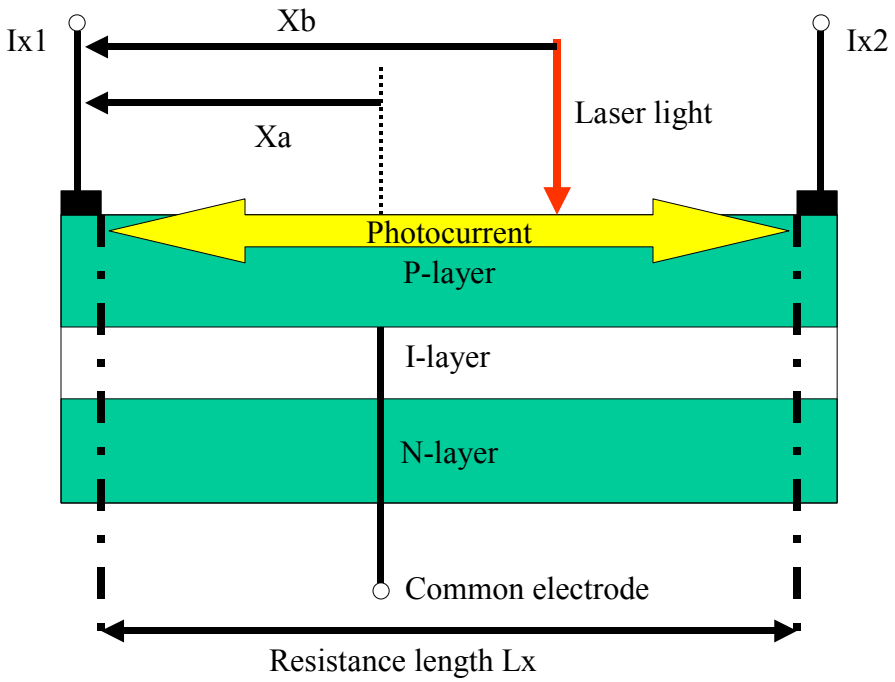

Figure 3. Cross-Section of 1-D PSD Detector Material

In the figure above, a P-type resistive layer is formed on a N-type high-resistivity silicon substrate. The P-layer is the active area for photoelectric current conversion. When light hits the PSD, an electric charge proportional to the light intensity is generated [Ref 4]. The electric charge is driven through the resistive layer and collected at the electrodes. The location of the light spot can be determined by dividing the photocurrent at each electrode (Ix_i) in inverse proportion to the distance between the incident position and each electrode [Ref 4].

$$\frac{Ix_1}{Ix_2} = \frac{Lx - 2Xa}{Lx + 2Xa}$$

The PSD outputs the center of gravity of the light, so the expanded beam is centroided to 500 nm, which is the best the PSD can resolve due to diffraction limit and the noise from it's power source and amplifier [Ref 3]

The PSD's used in this thesis are two-dimensional PSD's. This means that they measure the location of the spot on a horizontal and vertical axis of the PSD

detector face. The 2-D PSD has a resistive layer on the N-material and two electrodes connected to the N-material to provide Y-axis measurements. The P-material provides X-axis measurements on the PSD.

$$\frac{Ix_2 - Ix_1}{Ix_1 + Ix_2} = \frac{2x}{Lx}$$
$$\frac{Iy_2 - Iy_1}{Iy_2 + Iy_1} = \frac{2y}{Ly}$$

In this thesis, X and Y are going to be used to define another coordinate system, so PSD X and Y measurements will be referred to hereafter as f and g axes of the PSD.

4. Relevant Work Accomplished by Others

The most applicable research on this subject is being done in Korea under the sponsorship of Mando Corporation and Samsung. Park, Cho, Byun, and Park [Ref 5,6] have already solved the problem of optically measuring 6-DOF motion of a rigid body. Their implementation requires the use of a custom 3-facet mirror, an external laser, and three PSD's. The 3-facet mirror is attached to the center of the moving rigid body. 6 degrees of freedom are derived from using the mirror to split the single laser source into 3 beams. The 3 beams are read by 3 PSD's that have vertical and horizontal measurement capability. Three PSD's provide two measurements each--6 DOF is achieved.

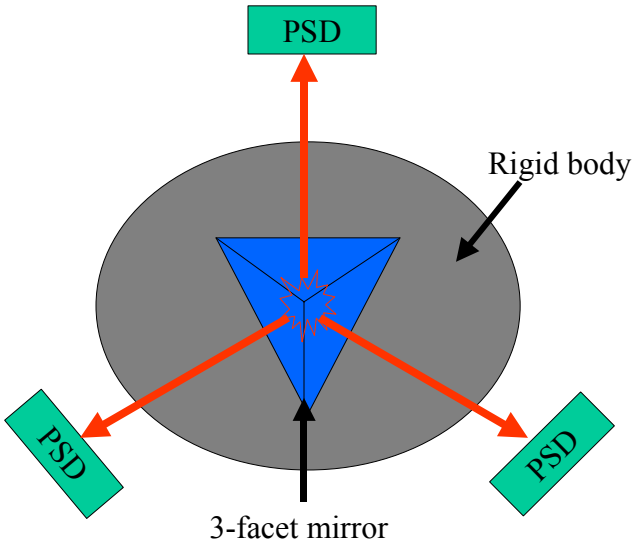

Figure 4. 3-Facet Mirror Metrology (viewed from external laser)

This implementation is excellent in the lab, but the requirement to have the source laser above the moving body would be undesirable for a spacecraft where real estate is at a premium. Also, the source laser would need to have a back-up because getting data on any of the degrees of freedom is tied to the reliability of a single laser.

The NASA Jet Propulsion Laboratory (JPL) [Ref 7] is conducting some very promising work. As a leader in space exploration, JPL is interested in precision instruments that are very light. The metrology system explored by the Koreans (and the metrology system built in this thesis) requires adding mass to the spacecraft and payload. The JPL approach minimizes the mass that must be added to the "payload" that is being controlled by using a small, light-weight, reflective diffraction grating. This allows for the heavy PSD's and laser to be off-board the payload—a very attractive option for an agile payload. The diffraction grating is a technique that should be considered in any future upgrade of the PPH metrology system.

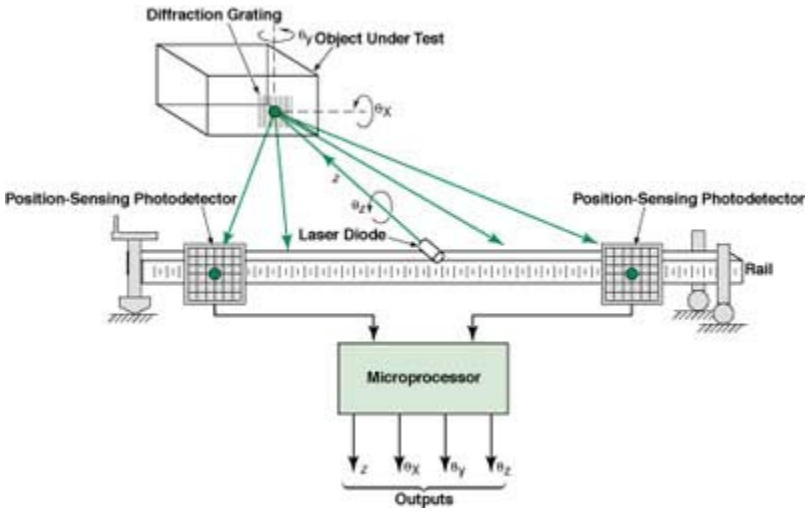

Figure 5. JPL Metrology System Using Diffraction Grating [Ref 7]

II. MATHEMATICAL REPRESENTATION OF THE SYSTEM

A. SYSTEM CONFIGURATION

The desired system configuration is three lasers and three PSD's in plane exactly 120 degrees apart with the spot from each laser hitting the origin of the PSD coordinate system. Putting the lasers in plane avoids the complicated analysis of "coning" of the beam intersection with the PSD. The 120-degree separation makes the geometry simpler since an equilateral triangle is formed. The advantages of this arrangement are that it is compact, it is easy to make and mount, it does not limit the travel of the moving plate, and individual motions are reasonably decoupled.

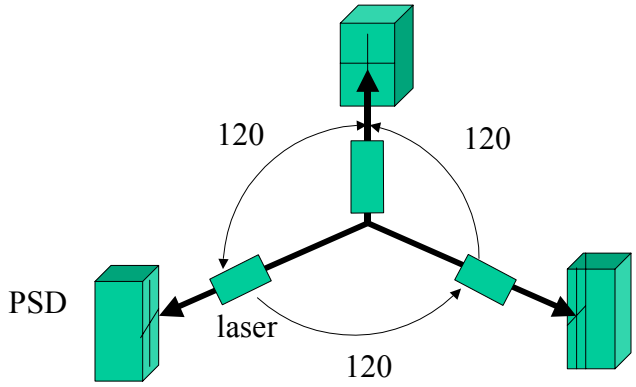

Figure 6. Ideal Laser Metrology Configuration

B. COORDINATE SYSTEMS

The PPH subsystem has its own local coordinate system for all of its components to be referenced against called the XYZ system. The XYZ system is fixed to the bottom plate of the PPH. If a spacecraft is used as the conceptual example, then it follows that the spacecraft has it's own reference coordinate

system that can be the same as the PPH bottom plate coordinate system or a different system probably near the center of mass of the spacecraft, X'Y'Z'. If the PPH is considered a subsystem to be mounted on the spacecraft, it would be mounted in reference to the X'Y'Z' coordinates. In this experiment, no outside X'Y'Z' system is identified, so the PPH is being treated as a self-contained subsystem with XYZ being the reference.

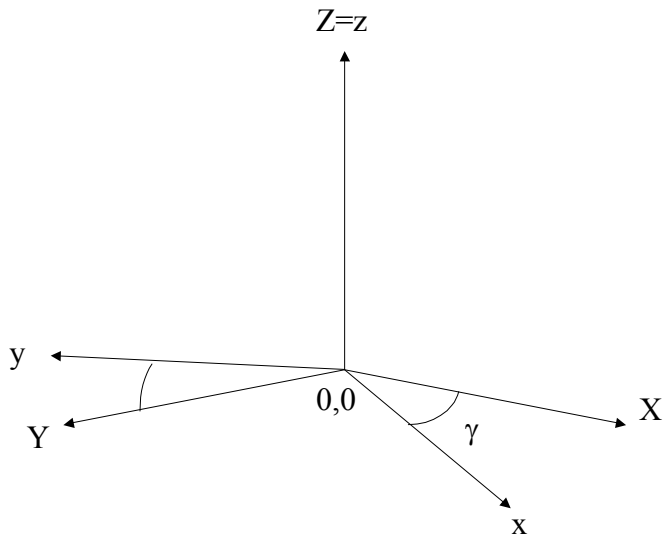

Figure 7. Offset Between PPH Bottom Plate Coordinate System and Metrology Coordinate System

The PSD's (xyz coordinate system) are offset from the X-axis of the bottom plate by an angle, $\gamma = -17^{\circ}$. The locations of the PSD's 120 degrees apart from each other are defined by another angle, α, measured counterclockwise from the x-axis in the x-y plane of the xyz system. The x-axis runs directly through the center of PSD1.

The top plate of the PPH is free to move in any direction and rotate about any axis. An additional set of coordinates, uvw, is tied to the center of rotation of the top plate. The lasers are attached to the uvw coordinate system and point at the PSD's located on the xyz system. The uvw=xyz when the there is no

translation or rotation away from the home position defined as the top plate level with the bottom plate and the lasers pointed at the centers of the PSD's.

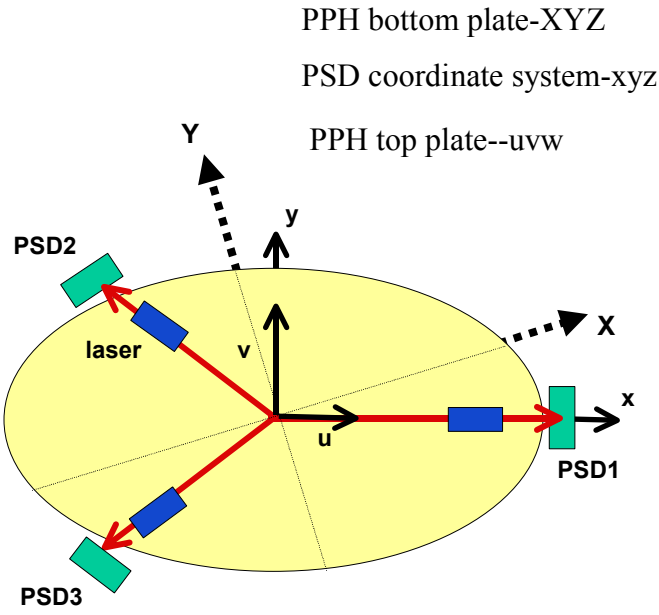

Figure 8. Relationship Between Laser, PSD and the Coordinate Systems

The PSD's detect the two dimensional locations of the spots formed by the laser beams intersecting the PSD detector surfaces. The locations of the laser spots (generated by top plate motion) are compared to known spot locations when the plate is at "home". This yields the position of the top plate in terms of the bottom plate coordinate system. Therefore, the translation (x,y,z) of the top plate and the rotation ($\theta_x, \theta_y, \theta_z$), can be determined by transformations that relate the PSD measurements to the translations and rotations that we are seeking.

C. SMALL ANGLE APPROXIMATION

The laser metrology system can detect angular travel of +/- 1.4 degrees from the home position and translation of up +/5 mm in the linear range of the detector. The small angle assumption allows for terms to be superimposed. Application of the small angle approximation also has the added benefit of

decoupling the measurements so that the matrix of transformations can be inverted to solve for the translations and angles that we really want to know.

D. APPROACH

The ideal case and small angle approximation allow for the problem to be split into two parts that are easier to visualize that can be added back together to get the final matrix. This involves looking at each individual small motion from the perspective of the PSD. The PSD can detect vertical and horizontal laser spot motion. In this analysis, the vertical axis of the PSD (laser spot motion normal to the bottom plate) is the f-axis, and horizontal motion is the g-axis.

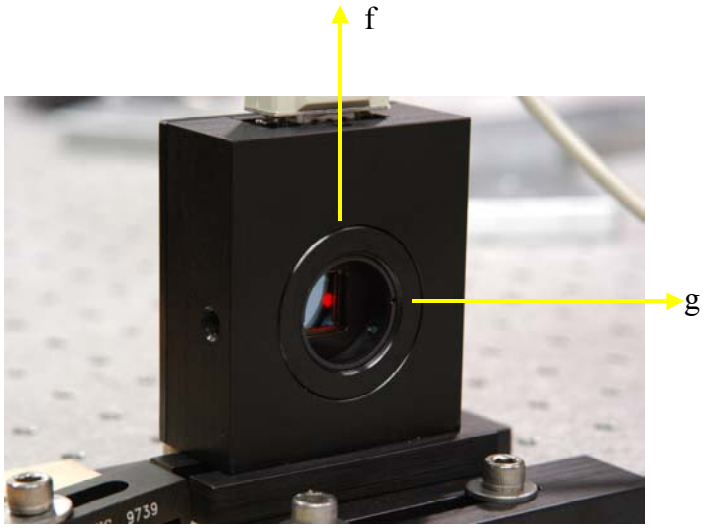

Figure 9. Annotation of f and g Axes on Actual PSD During Laser Alignment

The home position is when the top plate is parallel to the bottom plate. From this reference position any rotation about the z-axis, θ_z, or any translation in the x-y plane will generate non-zero g-axis readings while the f-axis reads zero. Therefore, x,y, and θ_z are determined as a function of the g-readings and are independent of the f-readings. Likewise, vertical translation out of plane, z,

as well as rotation, θ_x and θ_y, are only detected as f-readings on the PSD and are independent of the g-readings.

First, the results of positive rotation about x and y are evaluated from the perspective of the where the laser spot contacts the PSD. The vector, **e**, and its components are used to identify the location of the laser spot on the PSD. The vector, **e**, is fixed in length and is measured from the origin of the uvw system to where the laser spot contacts the PSD origin.

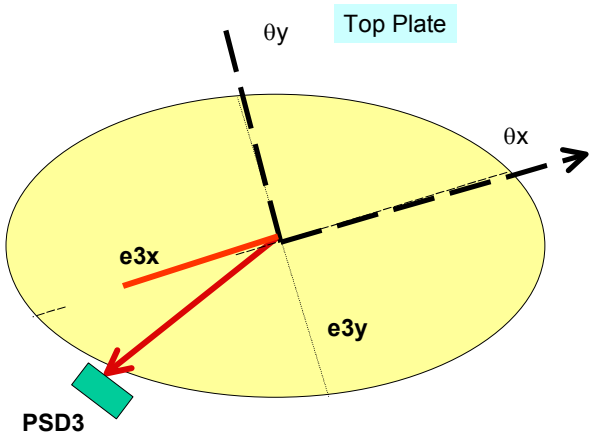

Figure 10. Resolving **e** into Components

A positive rotation about y results in a negative measurement along the f-axis. A positive rotation about x results in a positive measurement along the f-axis. By breaking **e** into it's x and y components an expression can be developed for $\tan(\theta)$ and $\tan(\phi)$. Translation along the z-axis is measured directly. For the rest of this thesis, e is the magnitude of **e.**

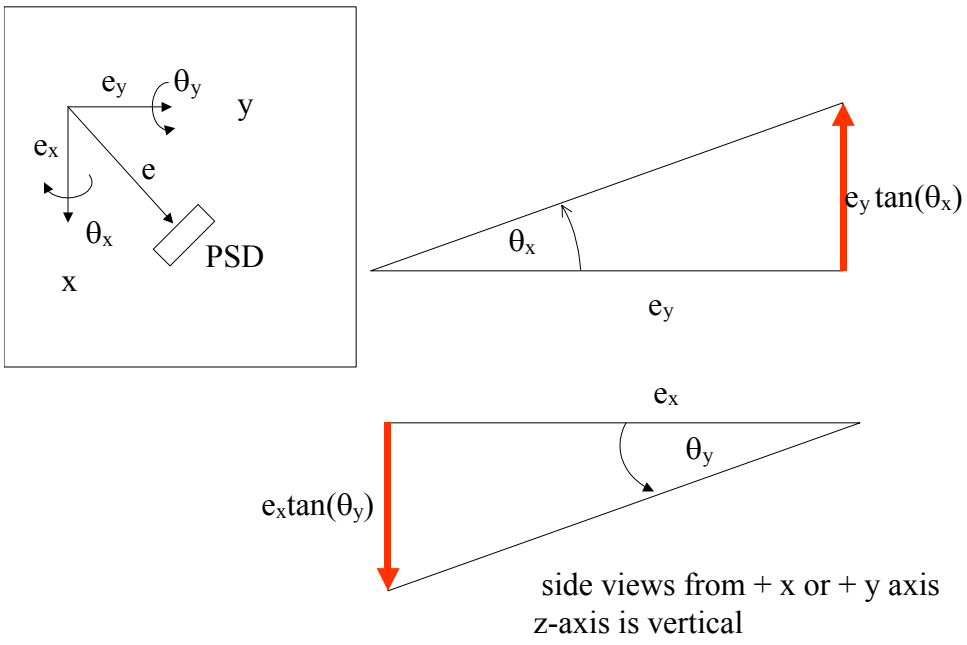

Figure 11. Decomposition of **e** and the Effect of Positive Rotations on PSD Readings

The relation between f measurements and $\theta_x, \theta_y,$ and z for small positive movements are

$$\begin{bmatrix} f_1 \\ f_2 \\ f_3 \end{bmatrix} = \begin{bmatrix} e_{1y} & -e_{1x} & 1 \\ e_{2y} & -e_{2x} & 1 \\ e_{3y} & -e_{3x} & 1 \end{bmatrix} \begin{bmatrix} \theta_x \\ \theta_y \\ z \end{bmatrix}$$

The tangents have been dropped from the angles due to small angle approximations.

The same process is followed for the g-measurements due to small motion in x,y, and θ_z. The diagram shows that θ_z is measured negatively in g.

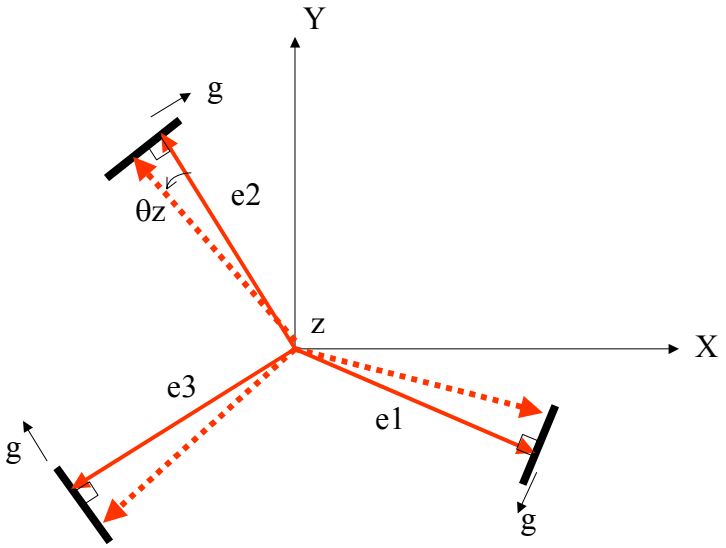

Figure 12. Top View of Positive Rotation About z

The expression for θ_z in terms of g is simply a function of the tangent

$$g_i = -e_i \tan(\theta_z)$$
$$i = 1, 2, 3$$

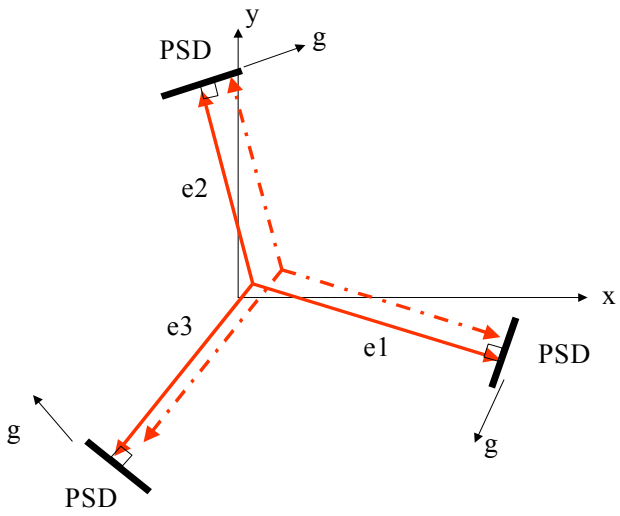

Figure 13. Top View of Positive x and y Translation

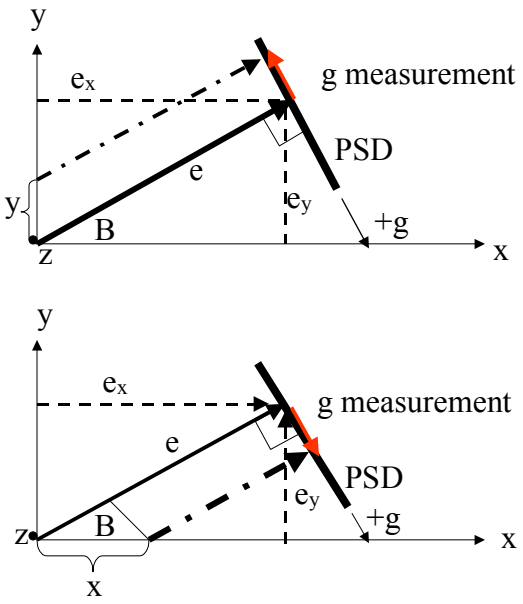

B is the angle between x-axis and **e** in +θz dir

Figure 14. Separating x and y Translation (Top View Down z-axis)

Translation in x is a function of the sine of the angle, β .

$$\sin\beta_i = \frac{e_{yi}}{e_i}$$

$$\cos\beta_i = \frac{e_{xi}}{e_i}$$

$$g_i = x\sin(\beta_i)$$

$$g_i = x(\frac{e_{yi}}{e_i})$$

$$i = 1,2,3$$

Likewise, translation in y is a function of the cosine of the angle, β .

$$g_i = -y\cos(\beta_i)$$

$$g_i = -y(\frac{e_{xi}}{e_i})$$

$$i = 1,2,3$$

The equations predicting g measurements for small positive movements in x, y, and θ_z are

$$\begin{bmatrix} g_1 \\ g_2 \\ g_3 \end{bmatrix} = \begin{bmatrix} \frac{e_{y1}}{e_1} & -\frac{e_{x1}}{e_1} & -e_1 \\ \frac{e_{y2}}{e_2} & -\frac{e_{x2}}{e_2} & -e_2 \\ \frac{e_{y3}}{e_3} & -\frac{e_{x3}}{e_3} & -e_3 \end{bmatrix} \begin{bmatrix} x \\ y \\ \theta_z \end{bmatrix}$$

Once again, the tangent has been dropped due to small angle approximation.

E. INPUT-OUTPUT RELATIONSHIP MATRIX

The results from the previous section can be collected into a matrix, L, to give the relation between small top plate movement and the PSD readings. In practice, the inverse matrix, $M = L^{-1}$, must be obtained to output the top plate location and orientation (x,y,z, $\theta_x, \theta_y, \theta_z$) from the PSD readings. The transformation matrix is the combination of the matrices for the expressions of f and g. The matrix below is useful for predicting what the readings in f and g should be on each PSD given small movements in x,y,z, and $\theta_x, \theta_y, \theta_z$.The inverted matrix in symbolic form is too large to fit in the body of this chapter, so only the numerical implementation is performed.

$$\begin{bmatrix} f \\ g \end{bmatrix} = L \begin{bmatrix} x \\ : \\ \theta_z \end{bmatrix}$$

$$\begin{bmatrix} f_1 \\ f_2 \\ f_3 \\ g_1 \\ g_2 \\ g_3 \end{bmatrix} = \begin{bmatrix} 0 & 0 & 1 & e_{1y} & -e_{1x} & 0 \\ 0 & 0 & 1 & e_{2y} & -e_{2x} & 0 \\ 0 & 0 & 1 & e_{3y} & -e_{3x} & 0 \\ \frac{e_{1y}}{e_1} & \frac{-e_{1x}}{e_1} & 0 & 0 & 0 & -e_1 \\ \frac{e_{2y}}{e_2} & \frac{-e_{2x}}{e_2} & 0 & 0 & 0 & -e_2 \\ \frac{e_{3y}}{e_3} & \frac{-e_{3x}}{e_3} & 0 & 0 & 0 & -e_3 \end{bmatrix} \begin{bmatrix} x \\ y \\ z \\ \theta_x \\ \theta_y \\ \theta_z \end{bmatrix}$$

$$\begin{bmatrix} x \\ y \\ z \\ \theta_x \\ \theta_y \\ \theta_z \end{bmatrix} = M \begin{bmatrix} f \\ g \end{bmatrix}$$

III. DESIGN

Now that the theory has yielded a solution to transform six measurements into the six degrees of freedom that we desire, it is time to consider the design of a system to support the geometry used to arrive at the solution. The Input-Output Relationship matrix, M, will be implemented in software. The laser and PSD geometry will be implemented with a mechanical system described in the following sections.

Designing and implementing the ideal metrology solution is not as straightforward as it might seem—the existing PPH hardware constrains what can be done. A decision was made to avoid any impact to the existing PPH, including disassembly. Therefore, the existing PPH was studied and measured to figure out how to arrange and attach the new metrology system to what already exists. The design team decided that the moving PPH top plate would host the lasers and that the PPH bottom plate would host the PSD's. Putting the PSD's on the moving portion of the PPH was considered, but the thick power cables to the PSD's were assessed to impair the motion of the plate.

A design decision was made to put the PSD's on a rigid, static frame at a fixed height and at 120-degree separation. The difficult part of building the support structure for the PSD's is the fact that the structure must not interfere with the PPH actuators. This drives the PSD support structure to be made from an ensemble of parts that must be toleranced and integrated.

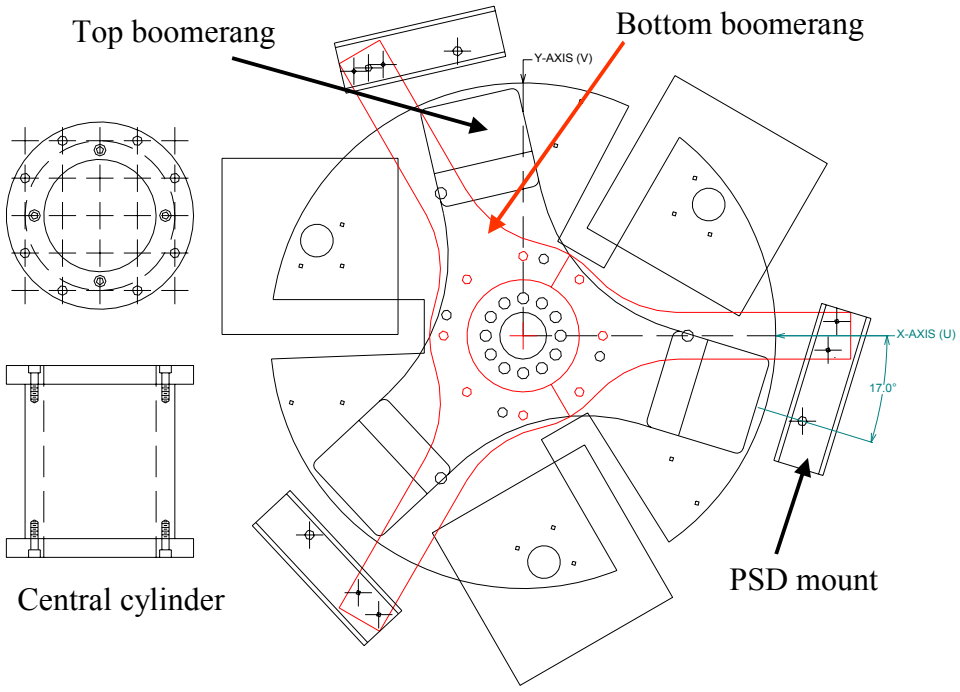

Figure 15. Design of Support System (Top View with Side View of Central Cylinder)

Starting from the ground and working up, a central cylinder attaches to the PPH bottom plate.

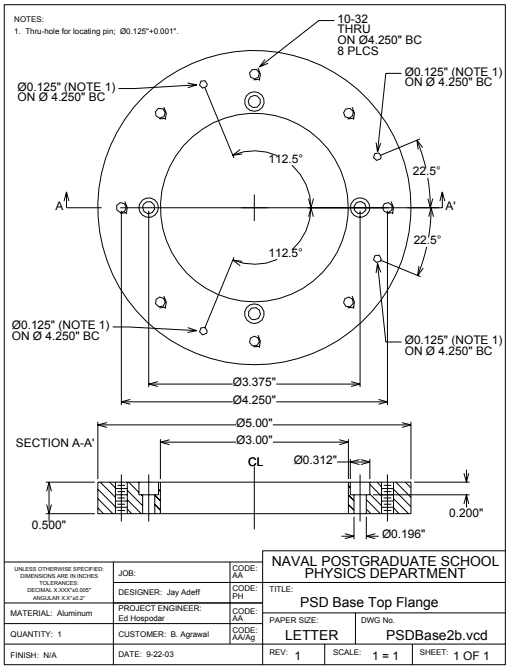

Figure 16. Top View of Central Cylinder Design

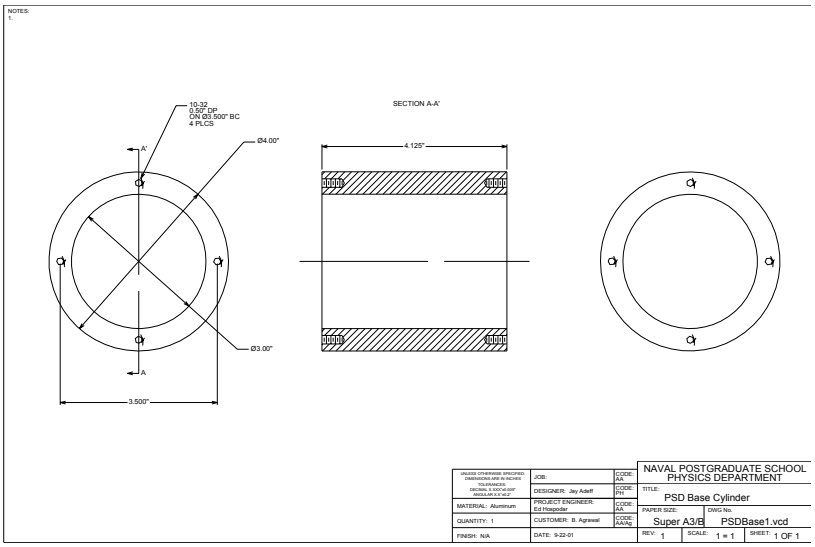

Figure 17. Additional View of Central Cylinder Design

The central cylinder supports the bottom boomerang which is manufactured in two parts to make it fit into the spaces between the actuators for assembly. The bottom boomerang provides the 120-degree spacing for the PSD's.

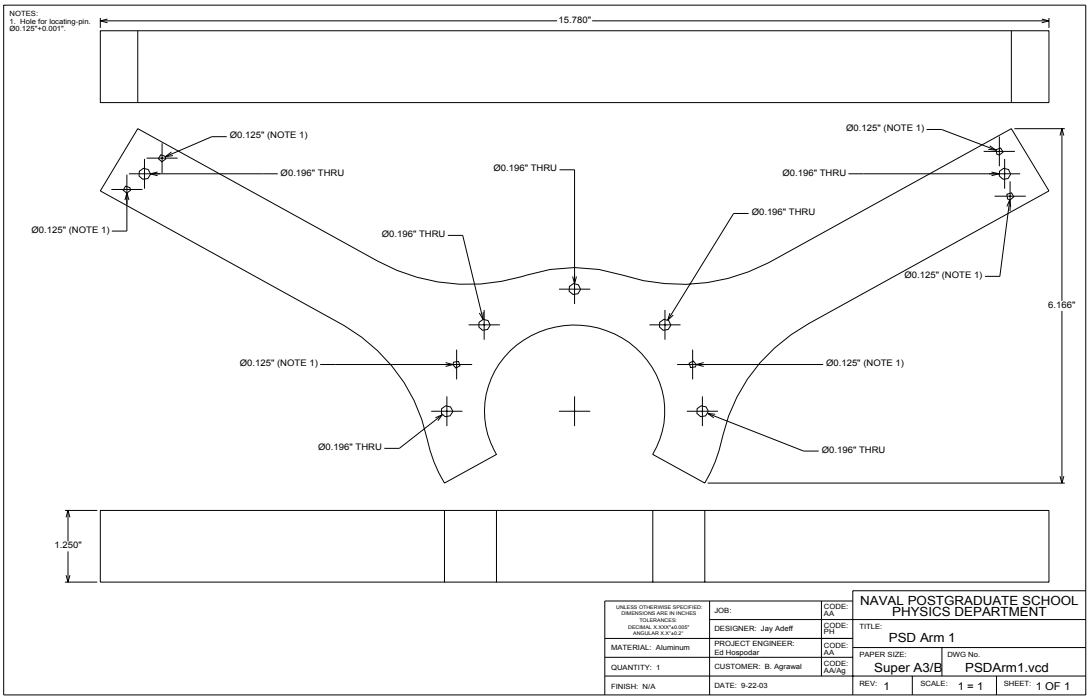

Figure 18. Design of Bottom Boomerang--2 Arms

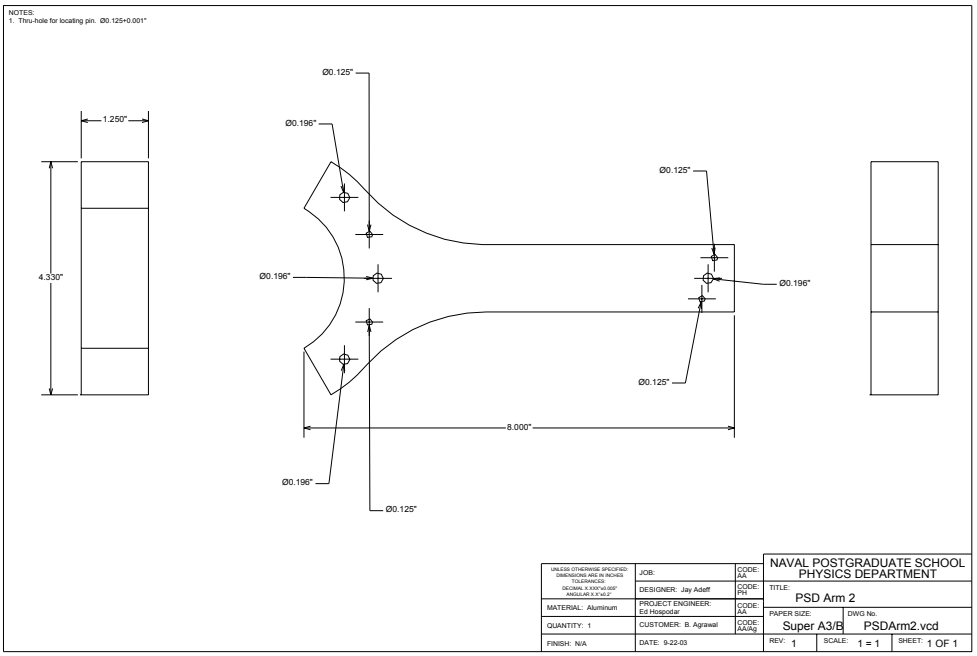

Figure 19. Design of Bottom Boomerang--1 Arm

The bottom boomerang supports the PSD mounts at the end of each arm. The PSD mounts hold the PSD's up to the level of the lasers.

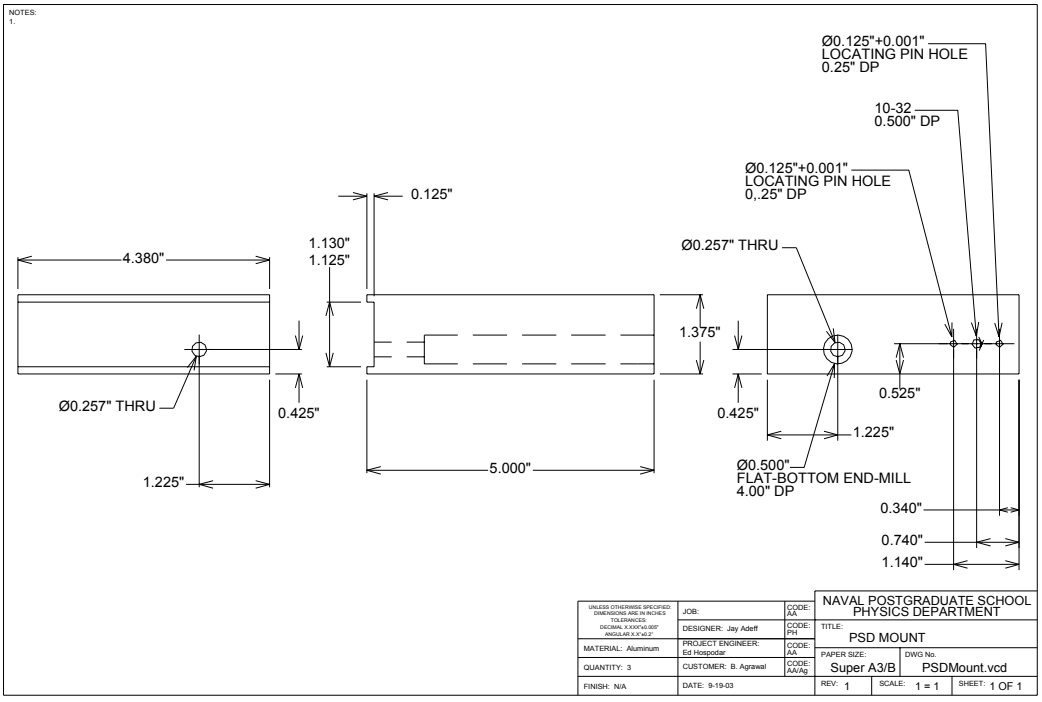

Figure 20. Design of PSD Mounts

The last part that attaches to the support structure is the bottom verification plate. It sits in the center of the bottom boomerang.

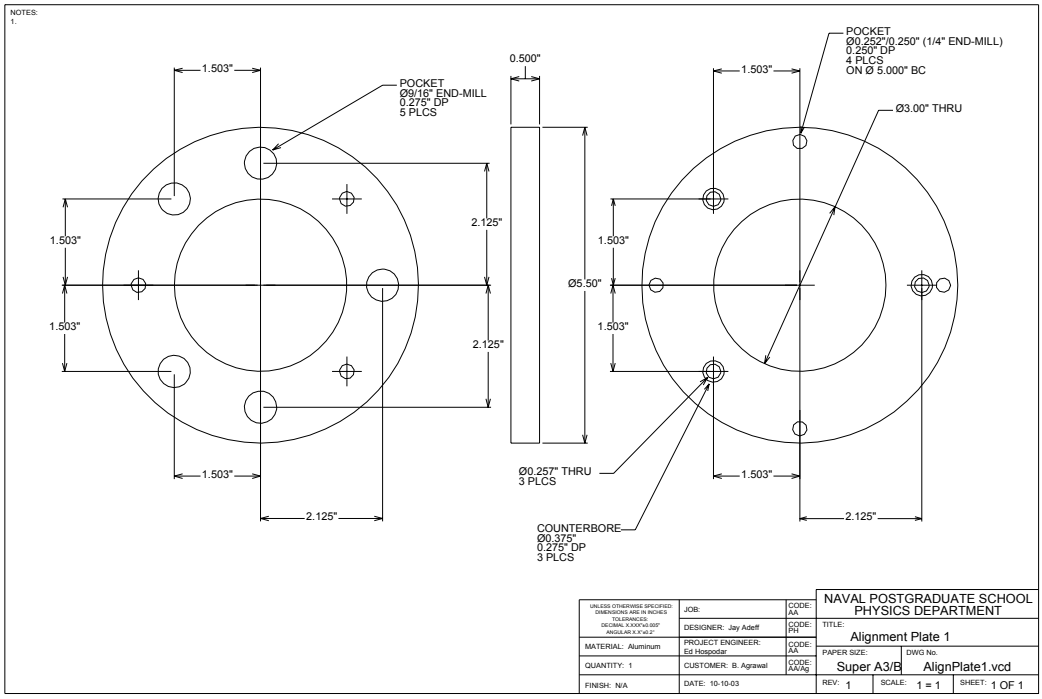

Figure 21. Design of Verification Base Plate

The moving top plate hosts the lasers on a smooth aluminum boomerang. The boomerang is necessary because the flatness of the PPH top plate is questionable because of its Plexiglas construction. The boomerang is designed to hold the three lasers in a level plane with 120-degree separation between each laser. The design of the boomerang points the lasers exactly at the centers of the PSD's when all translations and rotations are zero. Laser sleeves were designed to hold the lasers snug in the precision 4-axis mounts.

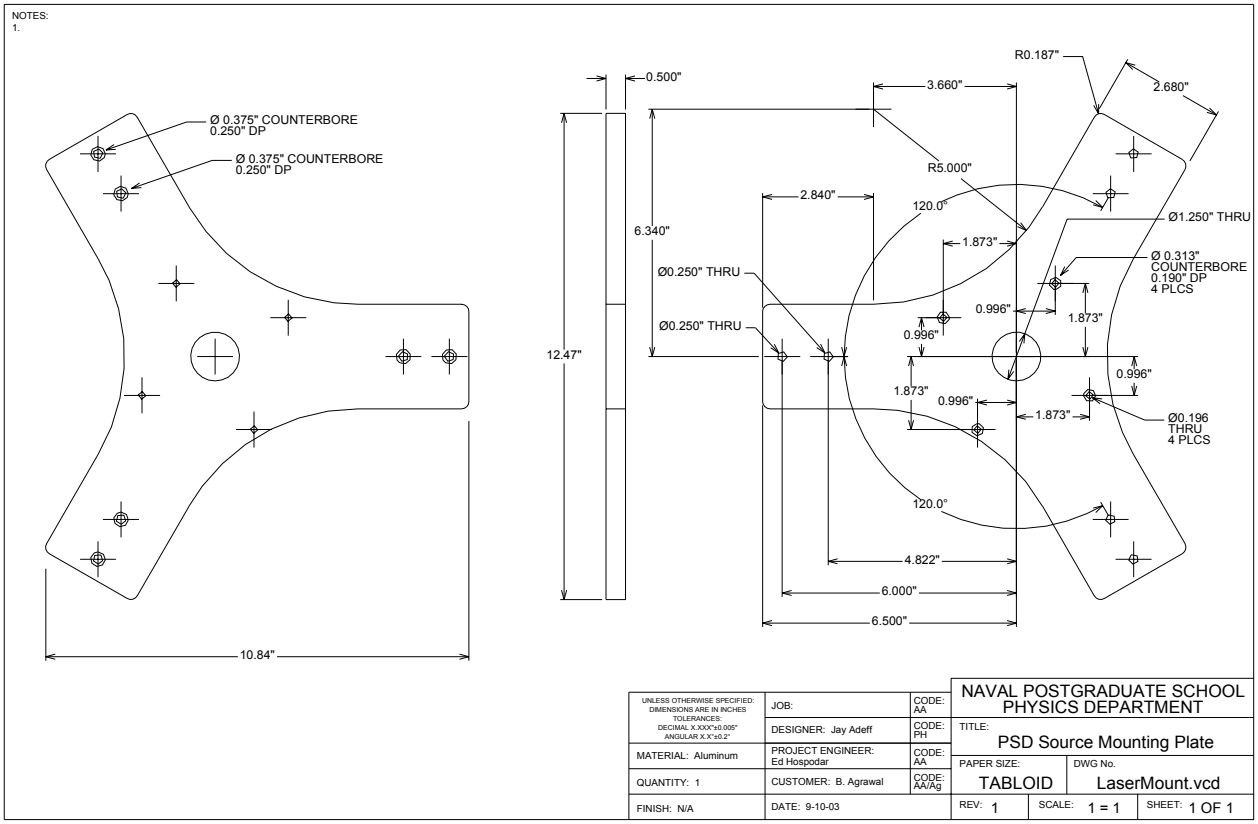

Figure 22. Design of Top Optical Boomerang

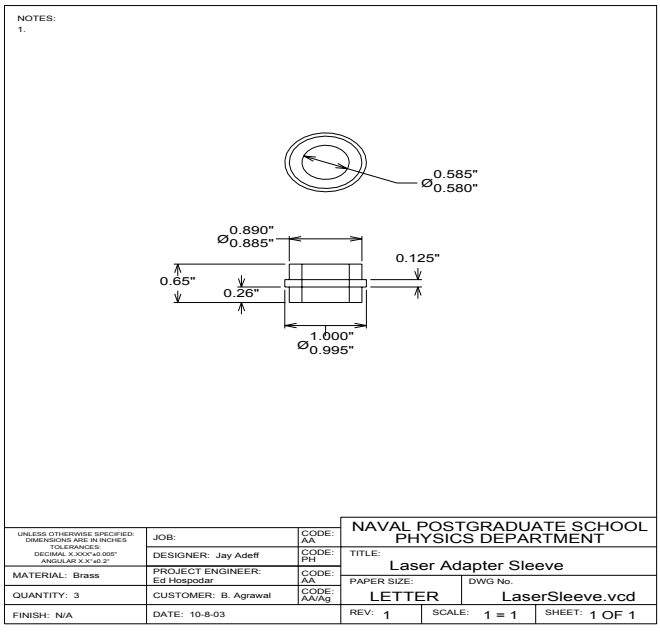

Figure 23. Design of Laser Sleeve

A verification system is also part of the design. Its purpose is to mechanically fix the top plate to a known location so that the real measurements can be compared to a known reference. The design includes attaching a base plate with 4 holes to the support structure (Fig 24) and a grooved plate to the underside of the moving top plate. Spacers of various heights connect the bottom plate to the top plate via the grooves and maintain the desired geometry. The geometries of interest are 0, 0.5, and 1 degree of rotation about x and y and 1 degree of rotation about z, and 0.2 inches in translation along x and y and 0.044 inches along z. Due to space constraints on the PPH and the realities of machining, the z-rotation needed its own plate, so 5-DOF are verified on one plate and 1-DOF is done on a separate plate.

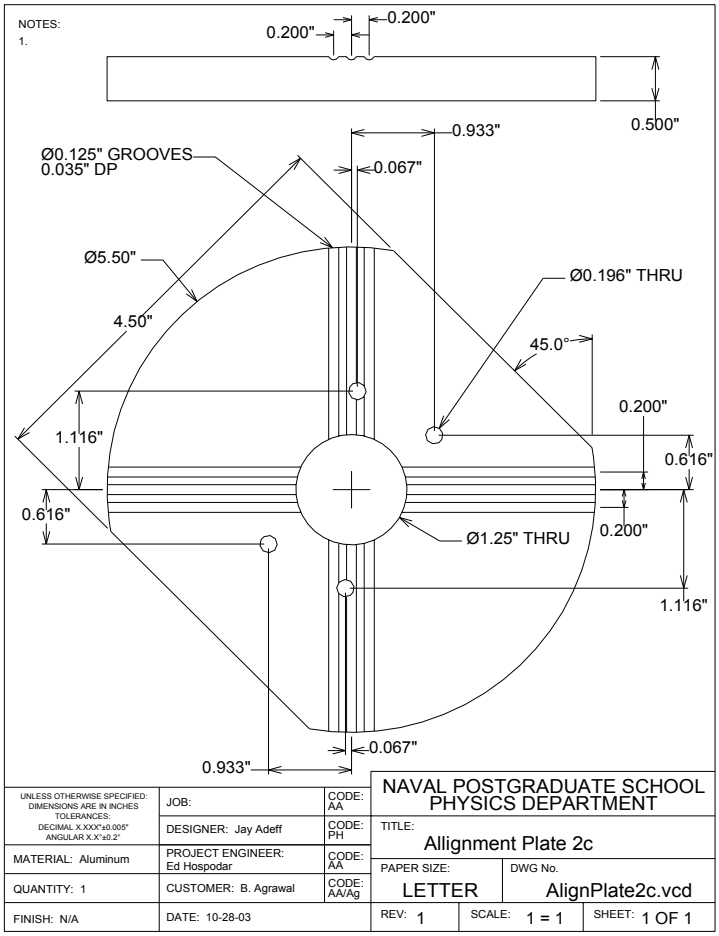

Figure 24. Design of 5-DOF Verification Plate

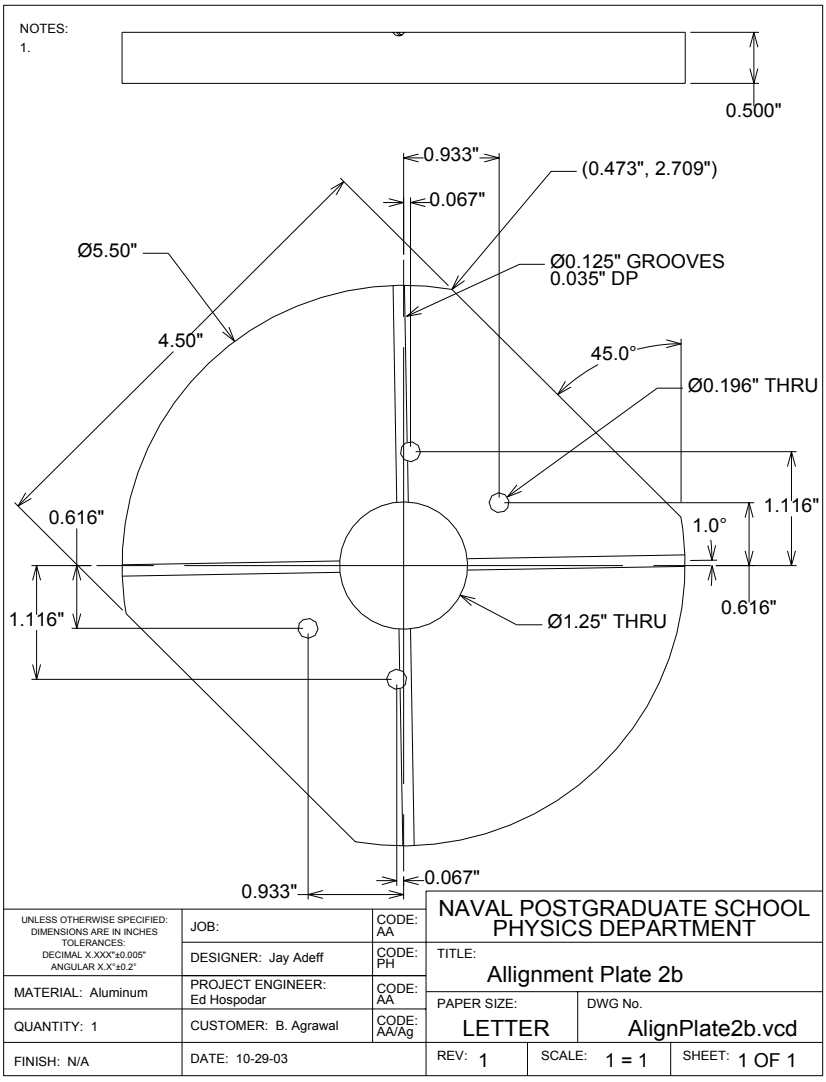

Figure 25. Design of 1-DOF Z-Twist Verification Plate

Verification Spacers come in different dimensions, but the design is the same, so one drawing can represent the family.

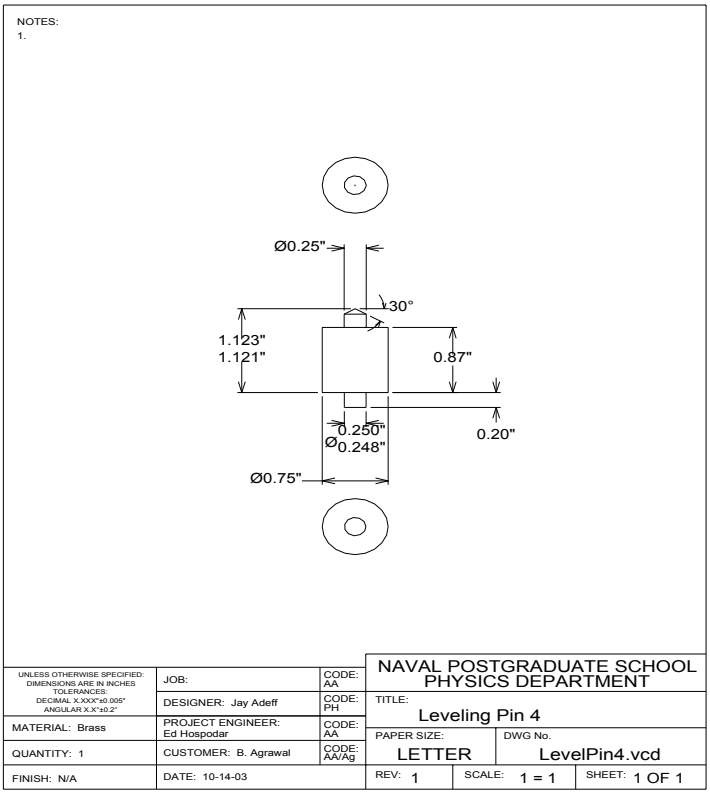

Figure 26. Design of Verification Spacer

THIS PAGE INTENTIONALLY LEFT BLANK

IV. HARDWARE FABRICATION AND INTEGRATION

A. LASER METROLOGY SYSTEM (LMS)

The hardware is designed to implement the ideal case on which the mathematical relationships were developed. In actuality, the fabricated items all have some errors. The hardware is acceptable if the fabrication errors are quantified and do not violate the assumptions in the mathematical relationships.

The laser metrology system consists of the laser subsystem and the sensor subsystem. The laser subsystem is composed of three main elements: laser, 4-axis precision mount, and top optical boomerang. The laser subsystem has 3 lasers set 120 degrees apart. The three lasers all lay in the same plane. The lasers sit in the mounts that are attached to the boomerang. The boomerang attaches to the moving PPH top plate. Cables connect the lasers to their power located off the PPH.

The sensor subsystem includes the PSD's, the support structure, and the amplifier. The support structure holds the PSD's level and vertical at 120 degrees separation. This allows the 3 lasers to point directly at the 3 PSD's when the PPH top plate is in its home position. The support structure is attached to the PPH bottom plate. The amplifier is located off the PPH and is connected to the PSD's by cables.

Additional equipment is used to initially align the lasers relative to their mounts and to provide a mechanical system of known angles and displacements to verify the mathematical relationships.

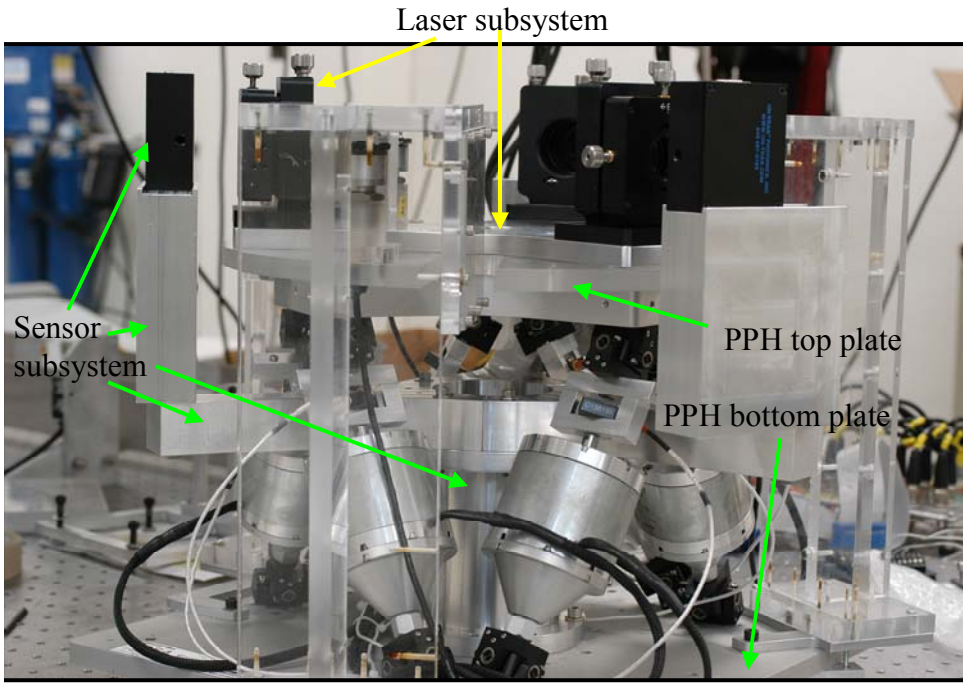

Figure 27. Laser Metrology System and PPH

1. Laser Subsystem

a. Laser

Figure 28. Diode Laser

The diode laser is the source of light energy that is to be detected on the PSD. Each laser is housed in a 4-axis precision mount.

vendor	Coherent
model	VHK2.3-5
quantity	3
wavelength	635nm+/-5
mode	CW
output power	4.9W+/-5%
spot size	1.1 mm
divergence	0.7 mrad
operating voltage	5-10 VDC
operating temp	-10 to 40 C
class	3a

Table 1. Laser Specs

b. 4-Axis Precision Mount

Figure 29. 4-Axis Precision Mount

The 4-axis precision mount provides the adjustment necessary to correct the accumulated errors in the laser metrology system. Adjustments help overcome imperfections in the fabrication that cause deviations from the design.

vendor	Coherent
part number	31-1605
quantity	3
x-y travel	+/-3.5 mm
x-y resolution	0.001 mm
angular travel	+/- 2 deg
angular resolution	7 arcseconds

Table 2. 4-axis Precision Mount Specs

c. Top Plate Optical Boomerang

The top plate optical boomerang is designed in an equilateral triangle with 3 arms separated by 120 degrees. It provides a flat surface (keeps laser mounts in a plane) and provides the necessary 120-degree angular separation. The top plate optical boomerang supports the 4-axis precision mounts and attaches to the Plexiglas PPH top plate.

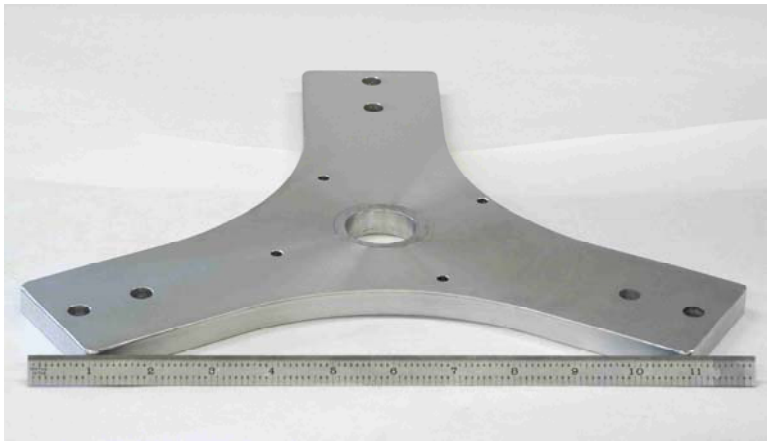

Figure 30. Top Optical Boomerang

machinist	Glenn Harrell
design	Jay Adeff
quantity	1
material	aluminum
angle separation between arms	
arm1 to arm2	120.0008 deg
arm1 to arm3	239.9969 deg
arm3 to arm1	120.0031 deg
thickness	0.5000 in
error	<0.0001 in

Table 3. Top Optical Boomerang As-Built Spec

2. Sensor Subsystem

a. Position Sensitive Detector (PSD)

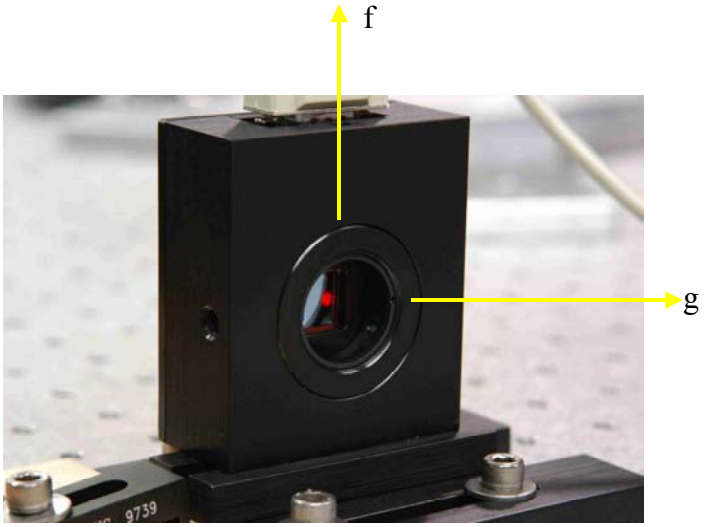

Figure 31. PSD

The PSD is the sensor that provides vertical and horizontal measurements of the incident laser light spot. It works on the same basis as a P-N junction (please see Background section for details). The PSD for this experiment is a dual-lateral PSD which means that the P material has 2 electrodes to make the x-axis measurements and the N material has 2 electrodes for the y-axis measurements. The vertical axis of the PSD will be referred to as the f-axis and the horizontal as the g-axis.

The PSD detector surface is 0.540 inches recessed from the face of the housing. This is important because the distance from the center of rotation of the top plate to the detector must be known accurately to calculate the small angles we desire.

It is also important to recognize that the PSD does not know the angle of arrival of the light. It only knows the size of the incident spot, so as the angle becomes large, the spot moves from a circular distribution to an elliptical distribution. Since the PSD centroids the light energy (see Background for details), light arriving at angles will have a different centroid than light arriving

from straight on. The small angle approximation allows for the assumption of a circular distribution of light. The PSD dimensions from the center of the detecting center to the side and bottom are 1.225”. The thickness of the PSD is 1.125”.

vendor	On-Trak
model	PSM 2-10
quantity	3
detector area	10x10 mm
nonlinearity	0.30%
responsivity at 940 nm	0.63 A/W

Table 4. PSD Specs

b. Support Structure

The support structure is made up of a separate central cylinder, optical boomerang, PSD mounts, and verification base plate. Since the central cylinder, boomerang, and verification plate were milled parallel and flat as an integrated assembly on the lathe, specifications for the subassembly are given instead of specifications for the individual parts. Specifications for the PSD mounts are given separately since they were milled individually.

Figure 32. Support Structure

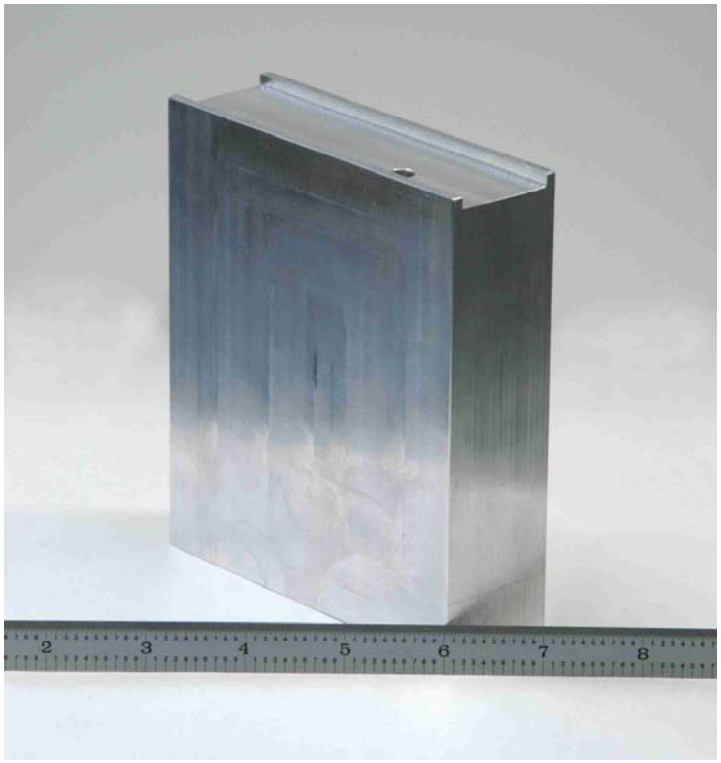

Figure 33. PSD Mount

(1) PSD Mount. The PSD mount is used to attach the PSD to the bottom boomerang. It attaches to pins on the bottom boomerang that project the PSD perpendicular to the support structure.

machinist	Glenn Harrell
design	Jay Adeff
quantity	3
material	aluminum
height of working surface	
mount 1	4.8680 to 4.8720 in
mount 2	4.8720 in
mount 3	4.8720 in
thickness	0.5000 in
measurement error	<0.0005 in

Table 5. PSD Mount As-Built Spec

The surface where the PSD attaches to mount 1 was not machined level. A piece of tape 0.003” thick (measured with a 1-2” micrometer with accuracy to 0.0001”) was applied to the uneven surface to shim it back to within 0.0001” of flat.

(2) Bottom Boomerang. The bottom boomerang has 3 arms designed to 120 degrees apart to coincide the 3 arms of the top optical boomerang. The bottom boomerang sits on the central cylinder and provides a level surface where the PSD mounts attach.

(3) Central Cylinder. The central cylinder provides a rigid pedestal that provides clearance for the bottom boomerang arms above the PPH struts. The base of the cylinder attaches to the CSA Engineering PPH bottom plate.

machinist	Glenn Harrell
design	Jay Adeff
quantity	1
material	aluminum
height of working surface	
arm 1	6.3740 in
arm 2	6.3740 in
arm 3	6.3740 in
angle separation between arms	
arm1 to arm2	119.989 deg
arm1 to arm3	239.989 deg
arm3 to arm1	120.010 deg
verification base plate	6.8590 in
measurement error	<0.0005 in

Table 6. Support Structure As-Built Spec

3. Support Electronics

a. Amplifier

The OT-301 provides power to the PSD, conditions the signals, and turns the photocurrent into an amplified output voltage that is fed to an A/D conversion in the hardware/software interface.

vendor	On-Trak
model	OT-301
quantity	3
sensitivity	10e-5 A/V
output	+/-10V
offset null	+/- 1V
linearity	+/-1%
calibration adjust	+/-10% of reading
power supply	12V DC

Table 7. Amplifier Specs

b. Laser Power Supply

The laser power supply is provided by three Coherent 5-10V DC power packs.

B. ALIGNMENT EQUIPMENT

The hardware below is used to align the lasers in their respective 4-axis precision mounts. The goal is to get the lasers level (no cants) and to center the laser in the mount. This is the extent of the alignment. The quality of the total metrology system alignment is the sum of the quality of alignment of the lasers in the 4-axis precision mounts plus the accuracy of the fabrication of the mechanical structures. This is discussed in detail in the Alignment and Verification chapter.

1. Optical Table

A 2-meter optical table was used to set up the alignment.

2. Optical Clamps

Various optical clamps and base plates such as the New Focus product shown below are used to build braces to secure the PSD in place on the optical table.

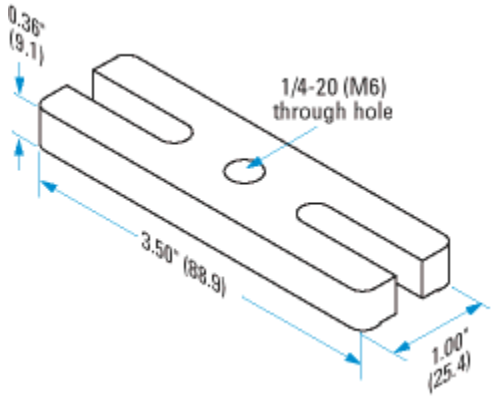

Figure 34. New Focus 9912 Base Plate.

3. Voltmeter

2 Fluke voltmeters connect to the amplifier to read out the f and g axis voltages of the PSD while aligning the laser.

vendor	Fluke
model	110
DC voltage range	0.1mV-600V
accuracy	0.7% of reading +2 counts

Table 8. Fluke Specs

C. VERIFICATION SYSTEM

1. Verification Hardware on the Moving PPH Top Plate

The verification system fixes the PPH in known positions so that the output of the metrology system can be compared to the predictions. Verification spacers of known height are placed between the grooves of the top verification plate and the holes in the bottom verification plate.

a. 1 DOF Twist Verification Plate

The twist verification plate is used to measure the twist about the z-axis. It is a separate plate from the other 5-DOF measurements because a 1-degree separation between etchings on the plates was not achievable by the machines in our machine shop. Therefore, two plates were devised, although this has the inconvenience of having to switch plate. Measurements would be better if every degree of freedom could be measured simultaneously from one fixed position. This necessity is a weakness of the verification system design.

Figure 35. 1-DOF Verification Plate

This plate is built to a thickness of 0.5130”+/-0.0005” and is parallel to less than within 0.0005”.

b. 5 DOF Verification Plate

The 5 DOF verification plate provides accurate reference positions for the PPH to known translations (x, y, z) and the rotations about x and y.

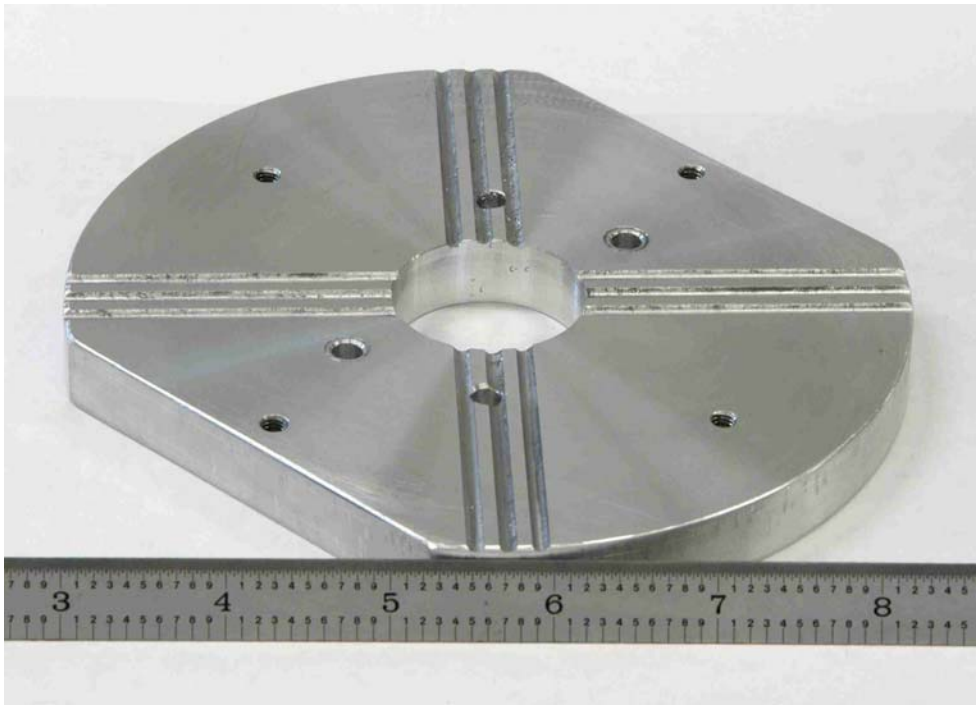

Figure 36. 5-DOF Verification Plate

This plate is built to a thickness of 0.5110”+/-0.0005”. The plate is parallel to less than 0.0005”.

2. Verification Hardware on the Stationary PPH Bottom Plate

a. Verification Base Plate

The verification base plate attaches to the bottom boomerang. The spacers sit in holes in this plate and connect to grooves on the other verification plates. This plate is discussed as part of the support structure.

b. Verification Spacers

Verification spacers work on the idea that there are 4 spacers arranged on the corners of a square. Two spacers are the same size and on

opposite corners, while 2 spacers of different sizes oppose each other on the other two corners forming a rigid ramp. The spacers can be combined in different groups to provide known angles of 0 deg, 0.5 deg, and 1 deg about x and y, and 1 deg about z.

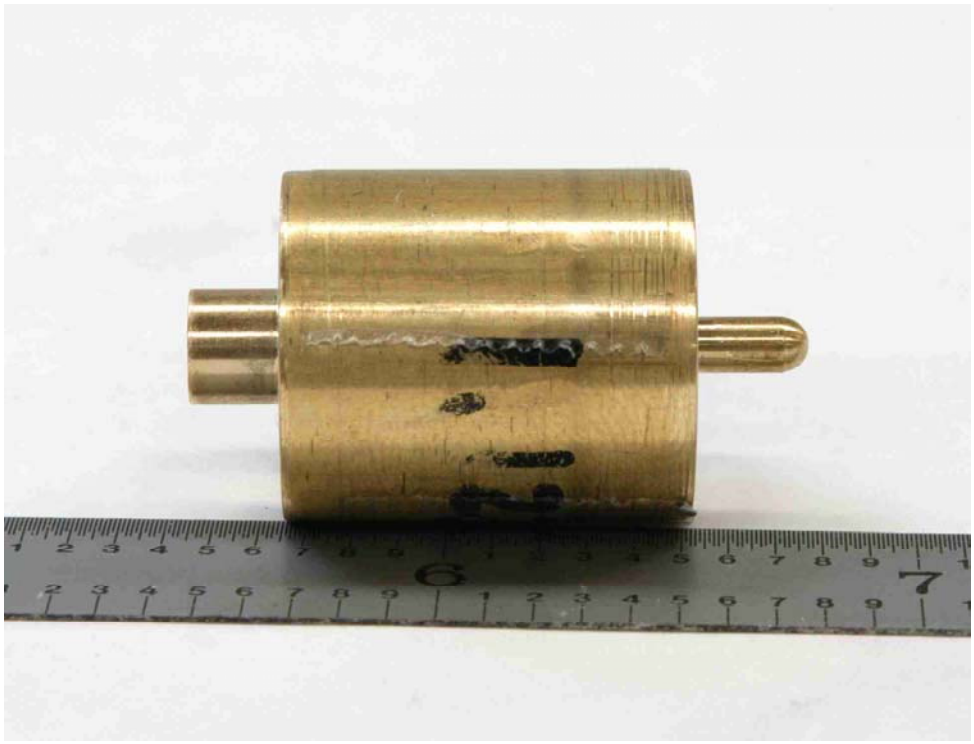

Figure 37. Verification Spacer

machinist	Glenn Harrell
design	Jay Adeff
material	brass
spacer size	quantity
1.057 in	1
1.079 in	1
1.123 in	1
1.101 in	4
1.145 in	4
measurement error	<0.001 in

Table 9. Verification Spacer Specs

V. ALIGNMENT AND INSPECTION

A. NEED FOR ALIGNMENT AND INSPECTION

The laser metrology system needs to be properly aligned so that the Input-Output relationships implemented in the software are valid for the design. Inspection (quality assurance) is required to determine how far the fabricated system deviates from the design.

The initial conditions of the design require that the three laser beams are: 1) in-plane 2) intersecting at a point, and 3) exactly 120 degrees apart with the three normal vectors to each PSD being 4) in a plane parallel to the x-y plane, 5) intersecting at the vertical axis of symmetry of the PPH, and 6) exactly 120 degrees apart. This constraints each laser to be hitting the normal to it's detector at the initial configuration (home position).

Aligning the lasers in their adjustable 4-axis precision mounts puts them in-plane (1) and is the subject of the next section. All other alignment responsibilities are a function of the rest of the structure. Since the structure cannot be adjusted, its contribution to the alignment of the rest of the system is dependent on the quality of the manufacturing. Deviations found during inspection are detailed in section C., and must be accounted for and corrected by the software.

B. ALIGNMENT

A precursor to doing any alignment is the choice of a known reference. The laser metrology system needs this reference so that deviations in alignment can be measured with respect to the known quantity. The reference for the laser metrology system is the bottom plate of the PPH.

The first step requires getting the lasers in plane. It involves making sure the laser points straight ahead and not canted off at an angle and then translating the laser to the center of the 4-axis precision mount. The best way to do this job would be to put the lasers in their mounts and secure them to the top optical

boomerang and then align all three lasers at once. A reference for this geometry was not readily available, so each laser and its 4-axis precision mount have been taken off the top optical boomerang and placed on an optical table and aligned in its mount independently.

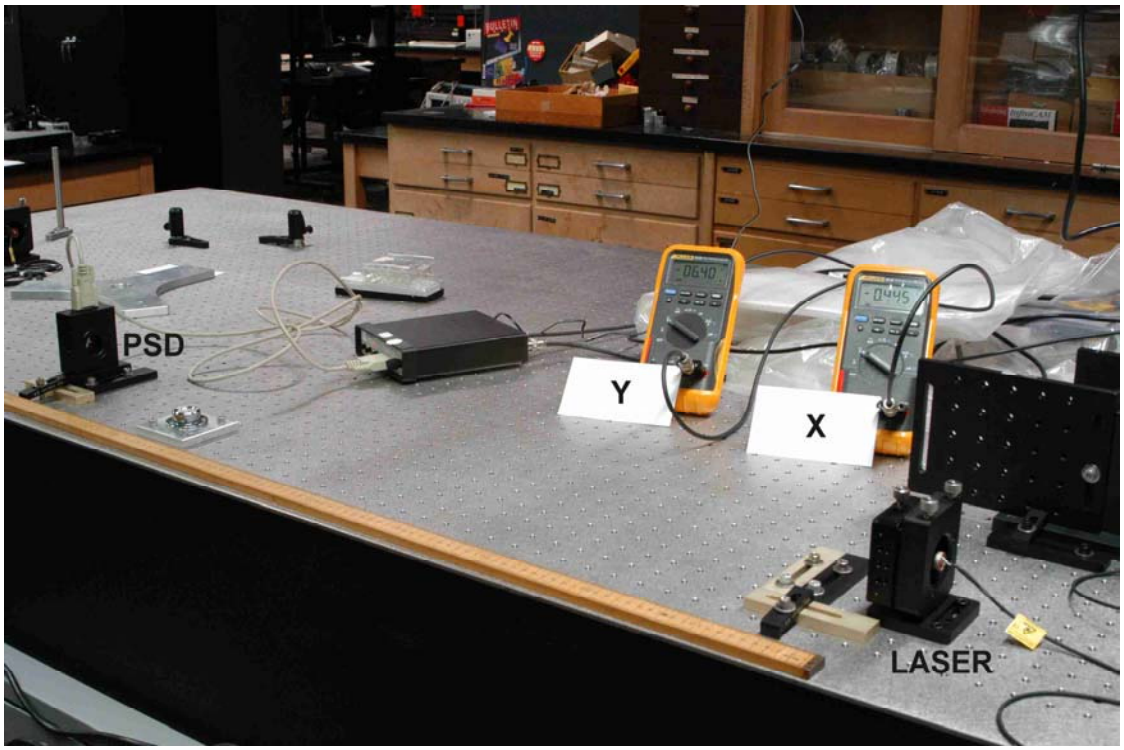

Figure 38. Optical Table to Align the Lasers Inside the 4-axis Precision Mount

The first step is to get the laser in the center of the mount. This is accomplished by taking a micrometer and centering the edge of the laser 23 mm (+/- 0.01 mm) from the top and side of each 4-axis precision mount. At this point the laser is in the middle of the mount, but it might not be pointed straight ahead due to the laser being canted up or down, left or right. Removal of the cant is accomplished by making the same laser beam hit the same spot on the PSD when the PSD is moved to two different locations as shown in Figs 39-41. The first measurement location, d_1, is 22 mm from the laser.

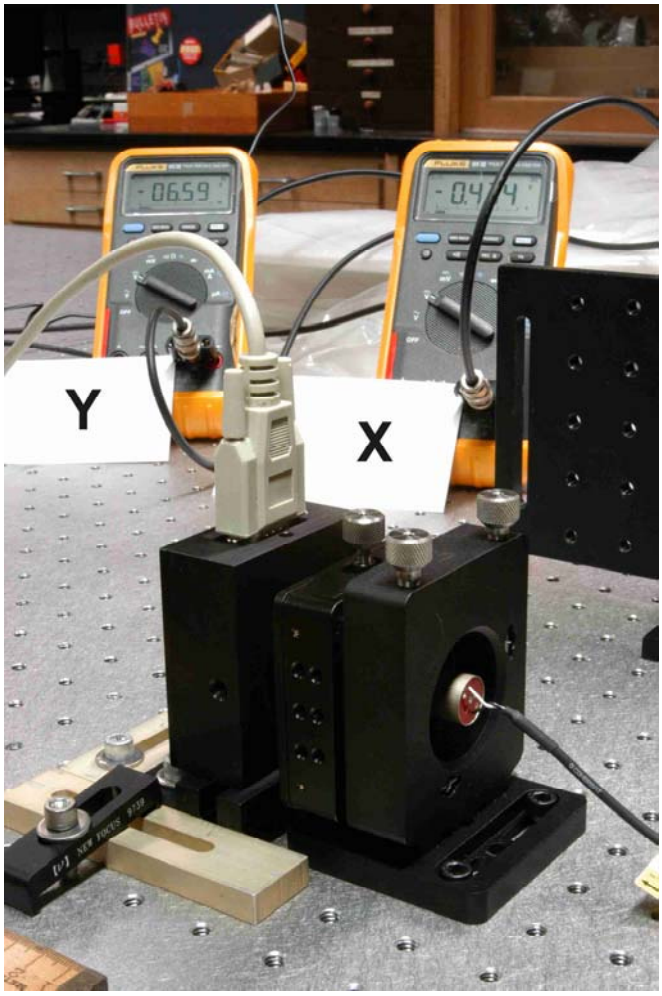

Figure 39. PSD located at d1, 22 mm from Laser. Voltmeters Read Spot Position

The second measurement location, d_2, is 985 mm from the laser. 963 mm separate each location. At each location the PSD is clamped with optical brackets to make it perpendicular to the table.

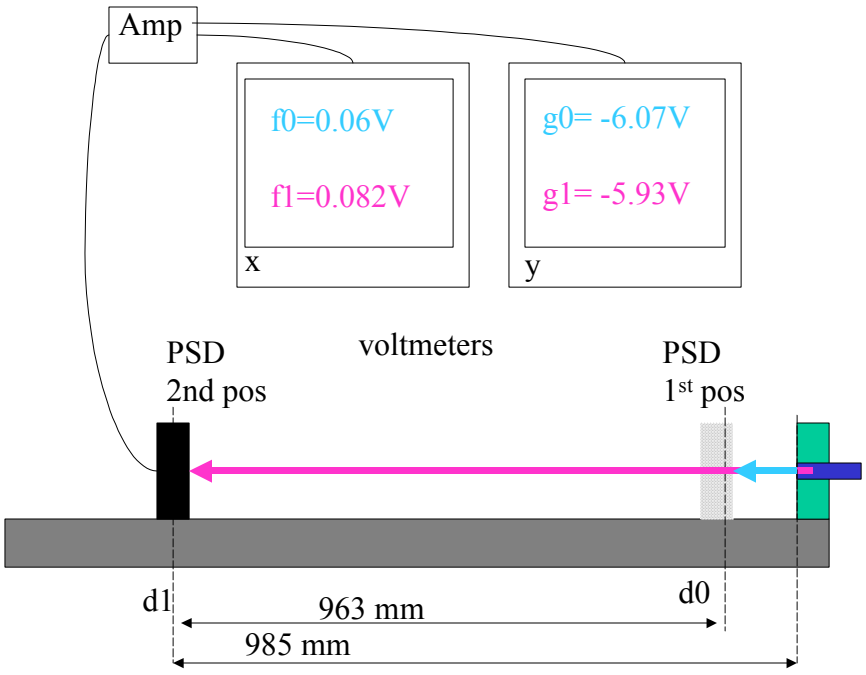

Figure 40. Alignment Bench

Removing the cants is an iterative process, where the output of each axis of the PSD is detected by a voltmeter. The vertical axis is leveled first by measuring the vertical voltage at both locations and adjusting the vertical cant knob on the PSD until the vertical voltage is almost the same at each location (within 0.0x V). The same is done with the horizontal voltage and horizontal cant knob at each PSD location The voltage can be read to the hundredth of a volt (noise made the thousandth position unsteady) which means that the spot location on the detector is known to 0.005 mm and the angle can be determined to no better than 0.00003 degrees over the distance of 963 mm. Once the laser is level in azimuth and elevation it is removed and another laser is aligned using the same method.

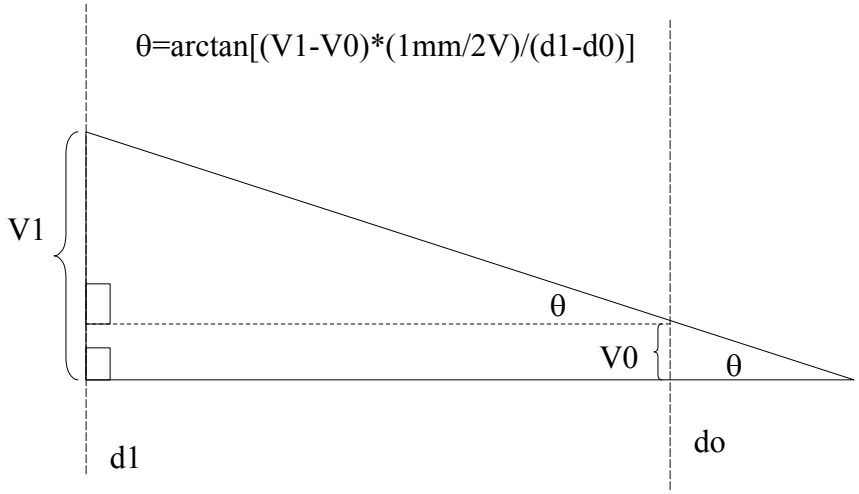

A voltage at 2 locations over a known distance yields the angle

Figure 41. Gunsight Alignment

Once all three lasers are initially aligned in-plane in their mounts, they are screwed back to the top of the top optical boomerang. The rest of the alignment rests with the integration of the structure and must be verified by inspection. Bias detected during verification can be accounted for in the software or removed by adjusting the horizontal and vertical knobs of the 4-axis precision laser mount.

	fo (V)	g0 (V)	f1 (V)	g1 (V)	Vertical angle error (deg)	Horizontal angle error (deg)
Laser 1	0.06	-6.07	0.082	-5.93	0.000654	0.004165
Laser2	-0.2	-6.27	-0.033	-6.22	0.003867	0.000259
Laser3	-0.451	-6.48	-0.422	-6.51	0.000863	-0.000892

Table 10. Alignment of Each Laser in Its Precision Mount

If the system gets out of alignment due to the violent motion of the PPH or human intervention, the entire alignment process mentioned above must be repeated to get the system back into alignment. In the future, it is desirable to be able to do alignment on the PPH. Solving this problem requires redundant beams or additional PSD locations. The most straightforward way would be to extend

the arms of the bottom optical boomerang so that there are additional PSD positions available to reproduce the process that took place on the optical table.

C. INSPECTION

1. Method of Inspection

The inspection strategy requires detailed as-built knowledge of the metrology system in the vertical and horizontal planes. The accuracy of the vertical integration of the structure affects the accuracy of θ_x, θ_y, and z because they are calculated from only the f-readings (vertical axis) of the PSD based on the small angle approximation. The accuracy of the horizontal integration affects x, y, and θ_z because they are calculated from only the g-readings (horizontal readings) of the PSD based on the small angle approximation. The structure supporting the PSD's is discussed first. The structure that supports the lasers follows. The rest of this section will discuss the inspection of these structures in terms of vertical and horizontal planes.

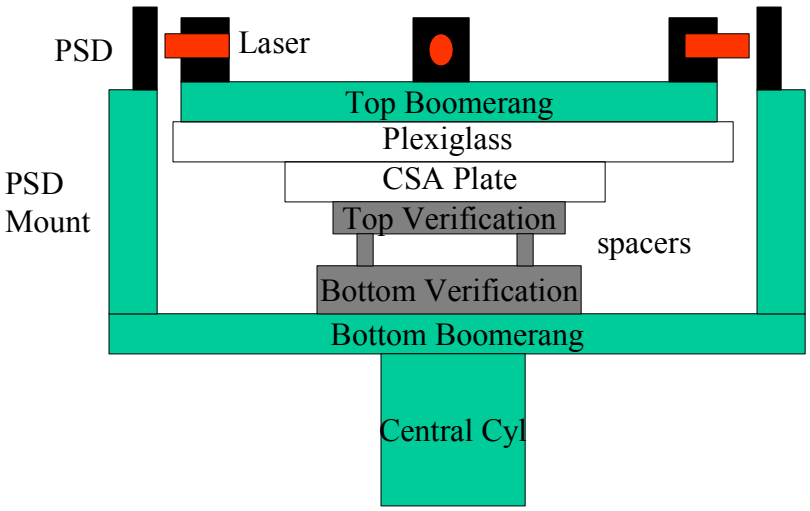

Figure 42. Vertical Build-up of the Structures

Each part fabricated by the NPS machine shop has been individually measured to determine the as-built dimensions and parallelness of every working

surface. Then the parts are assembled and the assembled structure is measured to determine its as-built characteristics. Measuring the errors of assembled structures is more important for the accuracy of the entire system than just measuring all of the piece parts because small things such as how much torque is applied to a connecting bolt can change the configuration a measurable amount.

2. Inspection of the Support Structure

The approach is to build up from the PPH bottom plate to the point where the PSD's are attached. The first sub-structure to go through verification is the assembly of the central cylinder, bottom optical boomerang, and the verification base plate.

Figure 43. Central Cylinder, Top Optical Boomerang, and Verification Base Plate Substructure. Precision Height Meter and Precision Granite Table also Shown

The two pieces of the bottom boomerang are bolted to the central cylinder and the verification base plate is bolted to the top of the boomerang. The assembly is then placed on the precision granite table where the height meter

slides along all of the working surfaces to determine the height and parallelness of the whole structure. The precision height meter is accurate to 0.0005”, but it is easy to ready halfway between each tick mark, or down to 0.00025”.

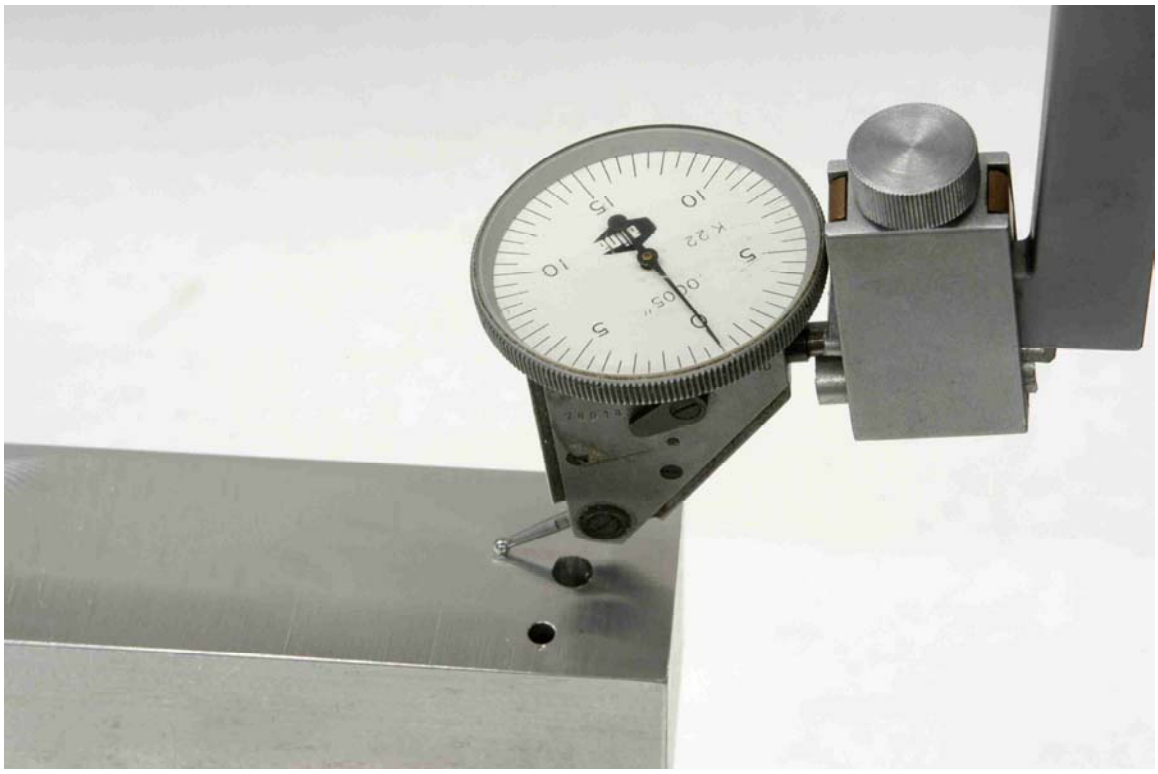

Figure 44. Precision Height Meter

Then the PSD mounts were added to the bottom boomerang and the top surfaces of each PSD mount was measured for height and parallelness. The tops of PSD mounts 2 and 3 (where the PSD’s will sit) are 11.2460” above the granite table. PSD mount 1 is 11.2420” above the granite table, so it is 0.004” shorter than the others.

Putting the PSD’s on their mounts is the next step. The measurements of the cylinder and boomerang substructure show practically no rotational errors. Therefore, the rotational errors are in the PSD’s attachment to their mounts. In order to check the 3 possible rotational errors of the PSD’s, the PSD mounts are taken off the support structure and attached to the PSD’s. Each PSD-PSD mount combination is then checked on the granite table. Noticeable errors manifest themselves in all three PSD-PSD mount combinations.

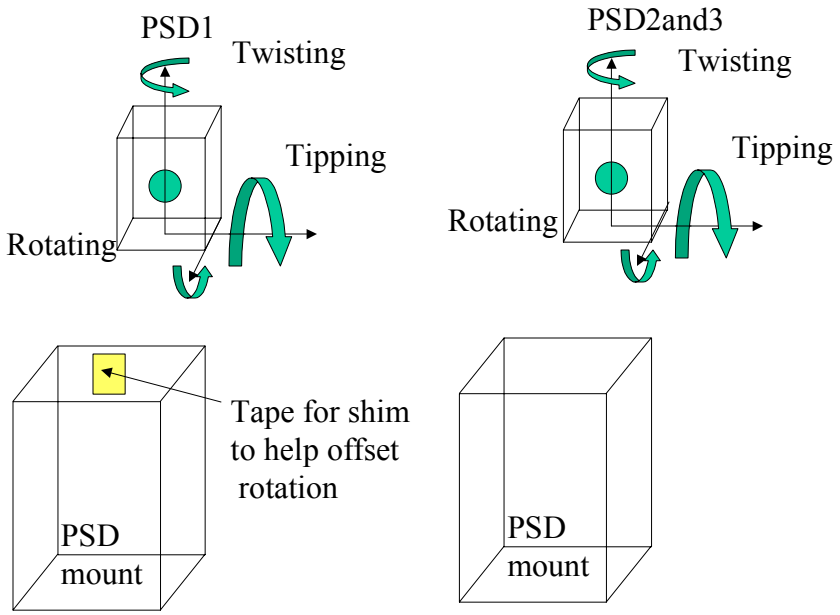

Figure 45. Errors Found When the PSD's are Attached to Their Mounts

The back cover of each PSD is not flush with the working surface. The back cover projects below the working surface 0.001" for PSD1 and 0.002" for PSD2 and PSD3, causing the PSD to lean forward toward the lasers (tipping). The angle of the lean and the affect of this lean on the vertical and horizontal locations of the detector origin are calculated by using the dimensions of the PSD. The equations showing the effect of lean are shown below. The effects of twist and rotation in the following sections are calculated in a similar manner but are not shown for brevity.

Thickness of PSD1=1.125". Back cover projection of PSD1=0.001"

$$\theta_{lean} = \tan^{-1}(\frac{deviation}{lengthofworkingsurface})$$

$$\theta_{lean} = \tan^{-1}\left(\frac{0.001"}{1.125"}\right) = 0.051\deg$$

$$\cos(\theta_{lean}) = \left(\frac{originlocation}{lengthofworkingsurface}\right)$$

$$\cos(\theta_{lean}) = \left(\frac{y"}{1.225"}\right)$$

$$y = 1.225"\cos(0.051) = 1.2249995"$$

The new origin vertical location is at y=1.2249995” The old origin location is at y=1.225”. The difference between the old location and the new location is 4.839e-7” or 1.2e-5mm. So this is a small impact, but must be added to the other errors discussed in the next paragraphs.

The next thing measured is twisting about the f-axis of the PSD. This is done by laying the PSD-PSD mount combo face up on the table and running the height meter along the PSD. Each PSD is level to 0.0005” or 0.023 degrees of twist about the f-axis of each PSD. Twist affects the horizontal aspect of the design, but does not affect the vertical build up.

The last test involves standing the PSD-PSD mounts back up in the vertical position and moving the height meter on the top of the PSD along the g-axis. This measures the amount of rotation about the normal to the face of the PSD at the corner of the PSD. PSD1-PSD mount has a measurable error of 0.002”. This causes an angle of 0.0468 degrees and moves the vertical location of the origin down 0.001” (0.0254mm) and the horizontal location moves out –0.001” (0.0254 mm). This is a significant deviation from the vertical design compared to tipping. The aggregate of the as-built deviations can be seen in the following table.

Vertical Estimate								
		PSD1		PSD2		PSD3		
item	**Design (inches)**	**As-Built (inches)**	**difference (in)**	**As-Built (inches)**	**difference (in)**	**As-Built (inches**	**difference (in)**	**+/- (in)**
Build-up to PSD								
cylinder+bottom boomerang	6.375	6.374	0.001	6.374	0.001	6.374	0.001	0.0005
PSD mount	4.875	4.871	0.004	4.872	0.003	4.872	0.003	0.0005
(0,0) of detector	1.225	1.22399	0.00101	1.22499	1E-05	1.22499	1E-05	0.0005
subtotal	12.475	12.46899	0.00601	12.47099	0.00401	12.47099	0.00401	0.0015
Build-up to Laser		Laser1		Laser2		Laser3		
cylinder+bottom boomerang	6.375	6.374	0.001	6.374	0.001	6.374	0.001	0.0005
verification baseplate	0.5	0.485	0.015	0.485	0.015	0.485	0.015	0.0005
verification spacer	1.1	1.101	-0.001	1.101	-0.001	1.101	-0.001	0.001
verification top plate	0.5	0.511	-0.011	0.511	-0.011	0.511	-0.011	0.005
groove in verification top plate	-0.035	-0.035	0	-0.035	0	-0.035	0	0.001
CSA plate+plexiglass	1.5	1.482	0.018	1.4905	0.0095	1.477	0.023	0.001
top boomerang	0.5	0.5	0	0.5	0	0.5	0	0.001
top boomerang to center of laser	2	1.9685	0.0315	1.9685	0.0315	1.9685	0.0315	0.0012
subtotal	12.44	12.3865	0.0535	12.395	0.045	12.3815	0.0585	0.0112
parallelism of verif system	0	0.00457	-0.00457	0.00457	-0.00457	0.00457	-0.00457	0.003
cant of beam	0	0.000352	-0.000352	0.000468	-0.000468	0.000358	-0.000358	0.005
total	12.44	12.391422	0.048578	12.400038	0.039962	12.386428	0.053572	0.0192
diff of subtotals		-0.077568		-0.070952		-0.084562		0.0177
convert to mm		-1.9702272		-1.8021808		-2.1478748		0.44958
Actual PSD f-reading		-2.535	-2.4198072	-1.886	-1.8021808	-2.693	-2.5974548	
percent error		4.544094675		4.444284199		3.547909395		

Table 11. Differences Between Design and As-Built for the Vertical Plane

Some interesting observations can be concluded from this table. The first conclusion is that the basic design has an error because the laser is 0.035" below the center of the detector. This is caused by the grooves in the top verification plate being overlooked during the build-up. This is taken care of in the bias adjustment in the software. In the As-Built columns, the machining is quite good but PSD1 sits slightly lower than the other two. The yellow boxes are calculations (from the aggregate of all the structural measurements) of what the PSD's should read out if the system is powered up. The red boxes show the actual readings and the percent error is the difference between what is expected and what is actually observed. Although the percent error is small, it shows that there are still some errors unaccounted for. These can be attributed to the fact that the flatness of the Plexiglas and CSA plates could not be determined since we did not want to disassemble the PPH. Also, some errors could have been introduced when the lasers were screwed into the top boomerang if the lasers were bumped even slightly. The yellow boxes serve an additional useful purpose—they are used as biases in the measurements taken during the verification of the software in the next chapter.

The inspection of the horizontal plane is now addressed. Precision pins are used to measure if the bottom boomerang is separated by 120 degrees. An Etalon micrometer accurate to 0.0001” measures the separation between the pins. The Law of Cosines uses the measurement of each side of a triangle to determine the interior angles. If the angles are the same, then each leg is separated by 120 degrees. The same process is used to determine the separation of arms on the top plate. The data shows the bottom boomerang and top boomerang are not equally spaced 120 degrees and cannot be perfectly aligned. Also, the assumption that the lines connecting the apexes of the triangles to the center of each triangle are all the same length is not verified. The assumption to use design data here mixed with inspection data is probably the source of some small errors. Correction will require disassembly to measure these values.

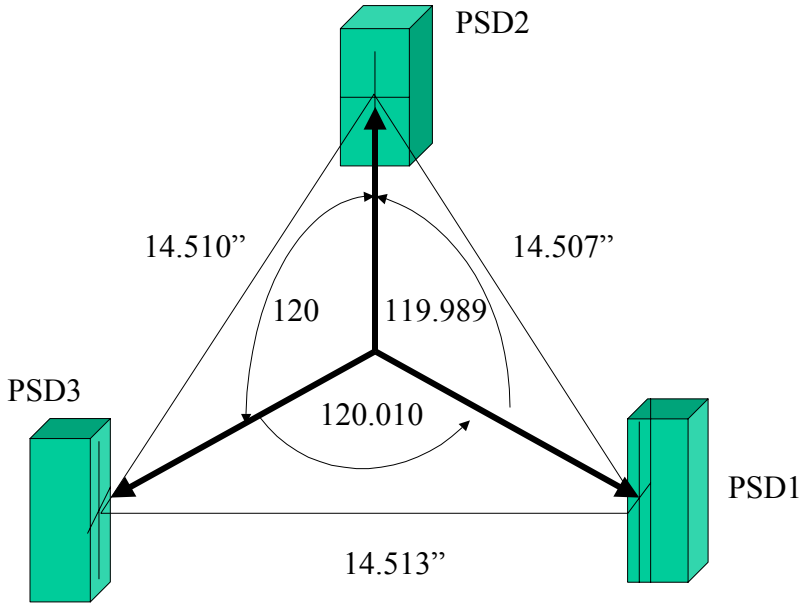

Figure 46. As-Built Angular Separation of Bottom Boomerang

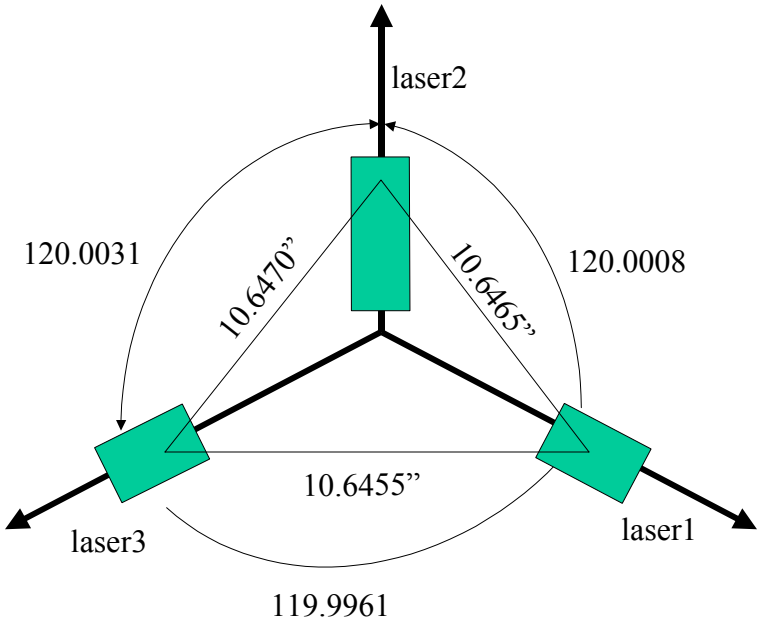

Figure 47. As-Built Angular Separation of Top Boomerang

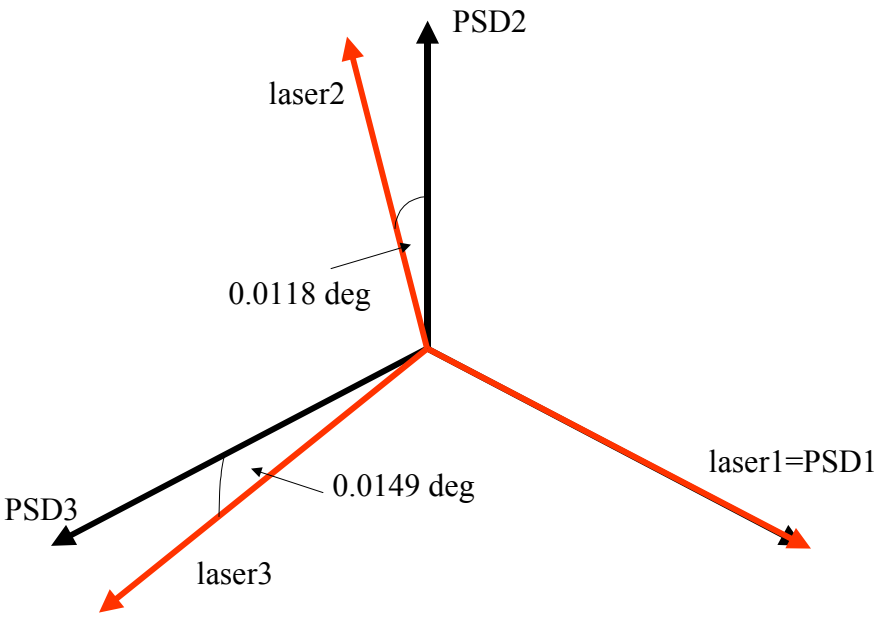

Figure 48. As-Built Alignment of the Top and Bottom Boomerangs

The precision 4-axis mounts are expected to be perfectly aligned on the arms of the top boomerang. This is not true. Measurements show that the screw

holes are slightly larger than the screws that attach the 4-axis precision mounts to the boomerang. Each mount is skewed clockwise (cw) or counter clockwise (ccw) from straight by up to 0.5 degrees. This is an extremely large source of error that causes a violation of one of the design conditions—all line intersect at a point in the center of the plane exactly 120 degrees apart. This is the largest source of error by an order of magnitude compared to other errors in the horizontal plane. These errors cause the lines to intersect in a region, not a point, and introduce problems with the calculation of angles because they deviate from the axis of rotation. It will be recommended that the top boomerang be given some kind of guides to make sure that the laser mounts screw into the boomerang straight.

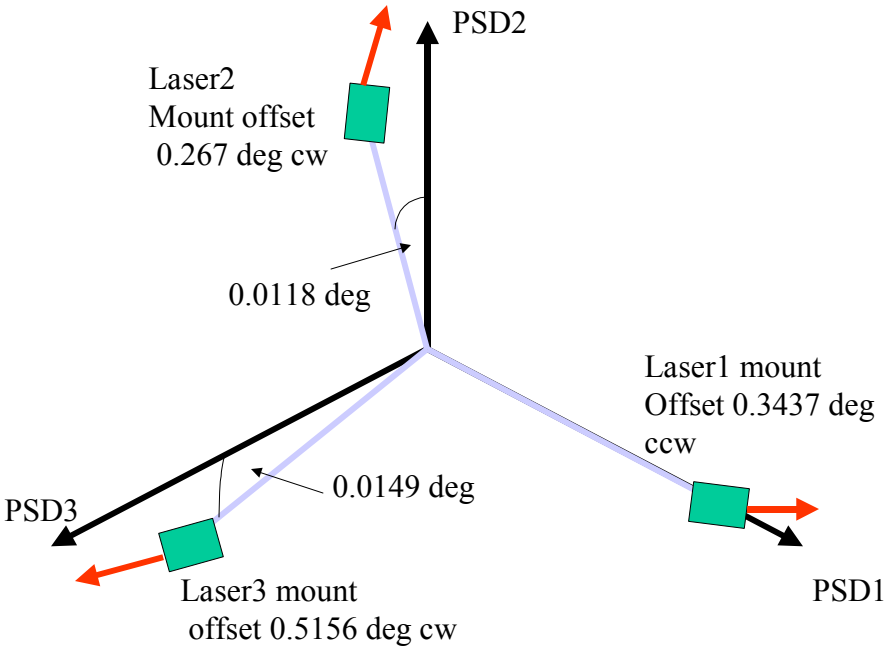

Figure 49. Summary of As-Built Errors Affecting the Ideal 120 deg Separation of Lasers and PSD's

The sum of these errors is shown in the following table.

Horizontal Estimate	Design (deg) wrt x-axis	As-Built (deg)	difference (in)	Design (deg)	As-Built (de	difference (in)	Design (deg)	As-Built (deg)	difference (in)
120 deg sep of PSD's									
bottom boomerang	0	0	0	120	119.989		240	239.989	
rotation	0		-0.001	0		-0.001	0		-0.001
twist of PSD about f	0		-1.64E-08	0		-1.64E-08	0		-1.64E-08
120 deg sep of Laser's									
top boomerang	0	0	0	120	120.0008	-0.001648	240	240.004	-0.00208
alignment of 4-axis mounts	0	0.3437	-0.0092	0	-0.267	0.0072	0	-0.5156	0.01386
alignment of lasers in mounts	0	0.004165	-0.000112	0	0.00149	0.00004	0	-0.000892	-0.000024
Verification									
sep of bot arm1 from top arm1	0	0.1	-0.0139	0	0.1	-0.0139	0	0.1	-0.0139
translation of grooves	0	0	-0.001	0	0	-0.001	0	0	-0.001
subtotal	0	0.447665	-0.025212016		-0.15371	-0.010308016			-0.004144016
convert to mm	0		-0.640385217	-0.663245217		-0.261823617	-0.284683617		-0.105258017
actual PSD f-reading			-0.656			-0.924			-0.197
percent error			1.104453744			69.19008479			34.96547383

Table 12. Differences Between Design and As-Built in the Horizontal Plane

This table (using the same verification setup as Table 10) shows that the calculated PSD readings and the actual PSD readings in the horizontal plane are not acceptable. The percent error is too large at PSD's 2 and 3. This means that assumption made to mix design data and inspection data are not valid for the horizontal axis. This will cause the readings of x, y, and θ_z to be untrustworthy until more inspection data is collected in the horizontal plane.

THIS PAGE INTENTIONALLY LEFT BLANK

VI. VERIFICATION

A. METHOD OF VERIFICATION

The verification of the Input-Output relationships is performed by a mechanical system attached to the bottom boomerang and the underside of the PPH top plate. The mechanical verification system consists of a set of plates and interchangeable spacers. The spacers firmly connect to grooves on the top verification plate to prevent slippage. The bottom verification plate attaches to the bottom boomerang, and it has holes for 4 spacers. There are two different top verification plates that attach to the PPH top plate. One plate has grooves cut in it to measure all the degrees of freedom except twist about z. A different top verification plate must be installed to produce θ_z. By selecting two spacers of the same height opposed from each other and by selecting two spacers of different heights for the other two holes, a triangle is formed at a known angle with the top plate on the hypotenuse. The angles selected for this experiment are 0.5 and 1 degree. Rearranging the spacers allows verification of θ_x and θy. Placing spacers of equal height and shifting the top plate allows for verification of x and y translation. Translation in z has a position at 1.101" and another at 1.145" for a total z translation of 0.044" or 1.11 mm. Switching top verification plates to the 1 degree offset allows for verification of θ_z This setup allows for tilting about each horizontal axis. It is important that the top plate not slip with respect to the bottom boomerang, so a pin-slot arrangement was crafted. Ideally, a larger range of angles and positions should be verified, but the necessities of time limit the verification to 0 degrees, 0.5 degrees, and 1 degree positions about θ_x and θy.

B. ACCURACY OF THE VERIFICATION SYSTEM

Errors in the verification system are due to machining. The machining errors have the effect of causing the true heights of the spacers to be off by 0.001 inches. This error in height affects the true angle of the calibrated position by the inverse tangent function. The as-built error of each plate is 0.00025" of parallel, so each plate can contribute 0.0036 degrees of error. The bottom

verification plate has its holes spaced 4.5 inches (114.3 mm) apart and half of this distance is used in to determine the angle of rotation:

$$\tan(\theta) = h/(b/2)$$
$$\theta = \tan^{-1}(0.001/2.25) = 0.025\,\text{deg}$$

The error in the calibrated position is this angle summed with the errors of the plate for a total of 0.032 degrees, so the accuracy of any measurement made by the laser metrology system is only good to 0.032 degrees. The precision of the laser metrology system is better than the accuracy of the calibrated reference positions. This means that the full capability of the laser metrology system cannot be realized in the existing physical architecture of the PPH. This should also be clear from the verification of the as-built accuracy of the hardware. A larger diameter verification base would allow for greater horizontal separation of the spacers and better verification. This would decrease the angular error even though the errors in the heights of the spacers would not have changed. A base of 22 inches would be required to get an order of magnitude improvement in calibrated angles. This is not feasible with the current physical setup due to space constraints. The other possible solution is to lap the surfaces. This would reduce the verification error to 0.000025 degrees—a three order of magnitude improvement.

Also, the verification plates may not screw into place in perfect alignment. This would cause a possible shifting error of +/- 0.001” of the screw holes and a possible rotation error of 0.1 degrees.

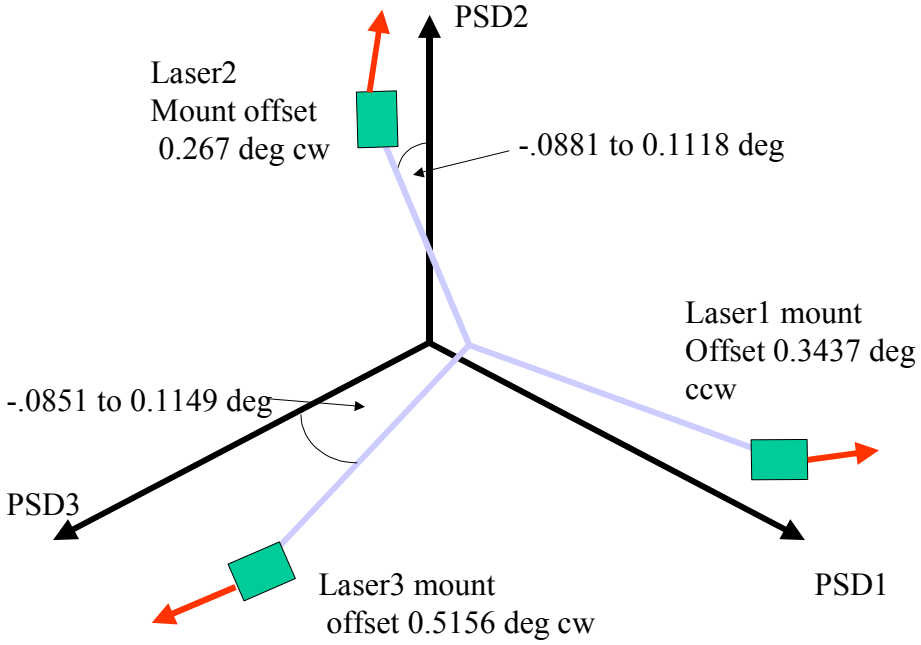

Figure 50. Additional Possible Misalignment of the Boomerangs Caused by the Verification Plates

During the verification process it became clear that the verification system is not sufficient for the job. First, it does not provide enough accuracy (it is not an order of magnitude more accurate than what it measures). Second, it is difficult to replace the pins and switch out the plates quickly. Third, it does not hold the plates securely. Calibration systems based on turning a precision screw to move a wedge or a commercially available sine plate are being considered as replacement designs for the verification system.

C. VERIFICATION RESULTS

The following table shows what the matrix expects for f and g on each PSD for each verification setup. The f readings incorporate the bias detected during inspection. The g readings do not incorporate any bias because knowledge of the horizontal aspect of the system is insufficient at this time. The data in bold show a situation where the bias has put part of the spot off the detector (limit is +/- 5mm).

verification settings	f1	g1	f2	g2	f3	g3
x=y=z=theta_x=theta_y=theta_z=0	-2.41	0	-1.8	0	-2.587	0
z=1.118 mm, all others =0	-1.292	0	-0.682	0	-1.469	0
theta_x=1.008 deg, all others =0	-3.4604	0	3.5007	0	-2.4503	0
theta_x=0.504 deg, all others =0	-2.9352	0	-0.0497	0	-3.8121	0
theta_y=1.008 deg, all others =0	**-5.8458**	0	-0.9918	0	0.0406	0
theta_y=0.504 deg, all others =0	-4.1279	0	-1.3959	0	-1.2732	0
theta_z=1 deg, all others =0	0	-3.5642	0	-3.5642	0	-3.5642
x= 1mm, all others =0	0	-0.2924	0	0.9744	0	-0.682
y= 1mm, all others =0	0	-0.9563	0	0.225	0	0.7314

Table 13. Predicted f and g Readings Using the Input-Output Relationship Matrix

Actual data is shown in the table below. Bold readings have been determined to be off the detector by visual inspection of where the spot hit the detector.

Actual data collected 3 Dec 03	f1	g1	f2	g2	f3	g3	x	y	z	theta_x	theta_y	theta_z
verification settings (1 var at a time)												
all = 0	-2.558	-0.722	-1.795	-1.045	-2.735	-0.381	-0.365	-0.118	-2.363	0.162	0.008	0.201
theta_y=0.504 deg	-4.237	-0.966	-1.442	0.362	-1.192	-1.009	0.882	0.178	-2.29	0.121	0.534	0.151
theta_y=1.008 deg	**-4.69**	-1.392	-1.23	0.934	-0.398	-1.4	-1.502	0.305	-2.106	0.083	0.733	0.168
theta_x=0.504 deg	-3.114	0.379	0.146	-0.926	-4.088	-0.996	-0.223	-0.866	-2.352	0.718	0.004	0.144
theta_x=1.008 deg	-3.534	1.167	1.625	-1.409	**-4.771**	-1.4	-0.506	-1.638	-2.227	1.098	0.048	0.15
z=1.118 mm	-1.397	-0.741	-0.696	-0.953	-1.4	-0.272	-0.351	0.197	-1.164	0.128	0.029	0.184

Table 14. Actual f and g Readings and Position and Orientation Calculated from Matrix

The actual data presents a mixed bag. It confirms the bias in the f readings, and the θ_z column suggests that the top boomerang and the bottom boomerang are misaligned by up to 0.201 degrees. It also shows that the lack of complete knowledge of the horizontal structure layout because g-readings greater than zero are shown where they should be zero. Also, data where the signal is partially off the detector incorrectly influences the calculations. Calculations in green show are within 10% of the predicted readings. Data in yellow exceed 10% error. The impression left by this data is that the Input-Output relationship matrix in the software is correct. Although the matrix can be tailored in the software, it would be best to fix the hardware.

RECOMMENDATIONS AND LESSONS LEARNED

Some difficulties in this thesis could have been anticipated, but they were overlooked, so hindsight is providing useful corrective guidance. This is all part of the learning experience, but students who wish to continue this work should not make the same mistakes so some recommendations and lessons learned are appropriate.

The first recommendation is to re-design the verification system. The verification system is not accurate enough (same order of magnitude) and is too difficult to use. A precision screw pushing a precise wedge or an off-the-shelf precision sine block or some other design would be preferable to the spacers.

The second recommendation is to fully inspect the structure—mixing even a little design data with inspection data corrupts the argument and makes verification very difficult because the problems cannot be easily isolated. Removal of as many unknowns as possible is an important part of determining accuracy. Therefore, the CSA top plate and the Plexiglas plate should be fully inspected and/or replaced by precision plates of known dimensions. This means disassembling the metrology system and the PPH (a design constraint we set up at the beginning of the process).

The third recommendation is to build templates to guide each part into the correct orientation for screws and bolts. The clearance between the screws and bolts and their holes causes significant misalignment of the laser mounts and the top boomerang. This also means that each top boomerang arm must have a reference surface to align against.

The fourth recommendation is to develop a scheme to align the lasers on-platform instead of having to do the alignment on a separate table leading to integration errors. This is a difficult problem, but the gunsight method might be feasible if each bottom boomerang arm was extended to hold a second PSD.

The last recommendation is to take the data again once the previous recommendations are implemented. This should yield much more accurate pointing knowledge.

Lessons learned during this thesis might help follow-on students. One of the biggest lessons is that any time hardware is involved the thought process that leads to the design must be well vetted and challenged early in the process. It is extremely difficult to backtrack or make corrections once metal has been bent. Thankfully, software can sometimes save the day. However, it is best to get the student, the draftsman, and the machinist together to make sure that what has been thought up can be designed to the constraints and that the design can be fabricated by the available tools and skill level in the machine shop. Almost forgotten basic engineering skills such as tolerancing, allowancing, and specifications on parallelism and dimensioning must be given a high priority in the drafting.

Even the best intentioned and agreed to plan will have hidden faults buried in it that will only become apparent down the road. This means that there must be significant schedule margin to accommodate redesign and additional quality assurance tasks.

Finally, doing a correct job requires keeping track of all the errors—it is the only way to know the accuracy. Designing an error budget during the systems engineering concept is a good way to anticipate where errors will come from and how to measure and handle them when they are uncovered during integration. Otherwise, the system will not have any absolute accuracy just relative precision.

LIST OF REFERENCES

1. Bishop, R.M. “Development of Precision Pointing Controllers With and Without Vibration Suppression For The NPS Precision Pointing Hexapod.” Naval Postgraduate School, CA, December 2002.

2. Taranti, Christian. “A Computationally Efficient Algorithm for Disturbance Cancellation to Meet the Requirements for Optical Payloads in Satellites.” PhD Dissertation, Naval Postgraduate School, CA, September 2001.

3. On-Trak Photonics. www.on-trak.com. December 2003.

4. Hamamatsu Corporation. www.hamamatsu.com. December 2003.

5. Park, W.S., H.S. Cho, Y.K. Byun and N.Y. Park.”Measurement of 6-DOF Displacement of Rigid Bodies Through Splitting a Laser Beam: Experimental Investigation.” Samsung Advanced Institute of Technology, Korea. November 2000.

6. Park, W.S., H.S. Cho, and Y.K. Byun.”Measurement of Vibrational Motions Using a Three-Facet Mirror.” Samsung Advanced Institute of Technology, Korea. December 2001.

7. Hochberg, Eric B. “System for Measuring Three Tilts and Distance of an Object.” NASA Jet Propulsion Laboratory, NPO-2106. November 2001.

THIS PAGE INTENTIONALLY LEFT BLANK

INITIAL DISTRIBUTION LIST

1. Defense Technical Information Center
   Ft. Belvoir, VA

2. Dudley Knox Library
   Naval Postgraduate School
   Monterey, CA

3. Brij N. Agrawal
   Naval Postgraduate School
   Monterey, CA

4. Hong-Jen Chen
   Naval Postgraduate School
   Monterey, CA

5. Andres Larraza
   Naval Postgraduate School
   Monterey, CA

6. Jay Adeff
   Naval Postgraduate School
   Monterey, CA

7. Glenn Harrell
   Naval Postgraduate School
   Monterey, CA